Am J Physiol Regul Integr Comp Physiol 290: R449–R455, 2006.
First published September 22, 2005; doi:10.1152/ajpregu.00684.2004.

Dietary NaCl supplementation prevents muscle necrosis in a mouse model of Duchenne muscular dystrophy

Mizuko Yoshida,[1] Akira Yonetani,[2] Toshihiro Shirasaki,[2] and Keiji Wada[1]

[1]*Department of Degenerative Neurological Disease, National Institute of Neuroscience, National Center of Neurology and Psychiatry, Tokyo, Japan;* [2]*Hitachi High Technologies, Ibaraki, Japan*

Submitted 5 October 2004; accepted in final form 13 September 2005

Yoshida, Mizuko, Akira Yonetani, Toshihiro Shirasaki, and Keiji Wada. Dietary NaCl supplementation prevents muscle necrosis in a mouse model of Duchenne muscular dystrophy. *Am J Physiol Regul Integr Comp Physiol* 290: R449–R455, 2006. First published September 22, 2005; doi:10.1152/ajpregu.00684.2004.—The mdx mouse is an animal model for Duchenne muscular dystrophy. Mdx mice fed a 12% NaCl diet from birth up to 20 days of age (mdx-Na mice) had an ~50% reduction in serum creatine kinase (CK) activity compared with mdx mice fed a standard diet. Most notably, necrotic fibers in tibialis anterior (TA) muscle of mdx-Na mice were reduced by 99% and were similar in control mice. These mdx mice displayed significantly elevated blood Ca^{2+} and Na^+ levels, while the total calcium content of their TA muscle was reduced to the level of control mice. In addition, mdx-Na mice had elevated zinc and magnesium contents in their TA muscle. These results suggest that elevated serum Na^+ leads to Ca^{2+} extrusion from muscle via the Na^+/Ca^{2+} exchanger causing a decrease in intracellular Ca^{2+} levels and an increase in blood Ca^{2+} levels. Extracellular Ca^{2+} and, in addition, Zn^{2+} and Mg^{2+} might also contribute to the stabilization of the cell membrane. Other possibilities explaining the surprisingly efficacious beneficial effect of dietary sodium exist and are discussed.

therapy; calcium and zinc; potassium; blood; serum creatine kinase activity

DUCHENNE MUSCULAR DYSTROPHY (DMD), a severe X-linked recessive muscle-wasting disease, is a health problem with an incidence of 2–3 per 10,000 males in the world population (15). The disease is caused by a defect in the gene encoding dystrophin, a protein located on the inner surface of the plasma membrane (44). The exact function of dystrophin is unknown, and the prospects for successful treatment of DMD remain uncertain, although numerous studies of gene therapy for DMD (21, 22, 42, 43) and of pharmacological treatment (8, 17, 23, 33, 37, 40, 46) have been published.

In DMD patients and in mdx mice, an animal model of DMD, the disease is characterized by necrosis of muscle fibers that causes increased serum levels of the muscle enzymes creatine kinase (CK) and pyruvate kinase (32, 48).

Dystrophin-deficient muscle membranes allow excess Ca^{2+} influx, causing calcium accumulation in necrotic muscle fibers (6, 11). The total calcium content of skeletal muscle fibers in DMD patients (3, 4, 24, 29) and mdx mice (19, 30, 34) is higher than that found in normal muscle fibers. The causes leading to excess Ca^{2+} influx into dystrophin-deficient muscle fibers are still unclear, although the following mechanisms have been proposed: *1*) because dystrophin is thought to have a mechanical function, dystrophin-deficient muscle fiber membranes are predisposed to rupture (2, 10); *2*) Ca^{2+} leak channels or stretch-activated channels open more easily in dystrophic myotubes, leading to poor Ca^{2+} regulation (18); and *3*) the function of L-type Ca^{2+} channels is abnormal (12, 47).

We found earlier that serum CK activity in mdx females more than 60 days of age is less than 50% of that observed in males in agreement with published observations (38). Also, we previously found that mdx mice given saline from ages 7 to 24 days exhibit significantly reduced serum CK activity by day 25. These interesting findings led us to ask the following questions: *1*) How does saline decrease serum CK activity and, presumably, prevent muscle necrosis in mdx mice? 2) Why is serum CK activity in mdx females lower in males? The answers to these questions may lead to effective therapies for halting the progression of DMD.

We hypothesize that *1*) saline may affect the concentration of some ions in the extracellular space (ECS), as well as in muscle fibers differently in mdx and control mice, and 2) these changes may be different between mdx female and male mice.

MATERIALS AND METHODS

Materials. Blood and tibialis anterior (TA) muscles of mice were used; mdx (C57BL/10ScSn-mdx) and control (C57BL/10ScSn; B10) mice were fed a standard diet (CE-2, Clea Japan, Tokyo, Japan) or a standard diet supplemented with 12% (wet wt) NaCl (NaCl diet). These mice are termed "mdx-Na" and "B10-Na." The diet containing 12% NaCl was given to pregnant mice beginning 2–3 days before delivery and continued throughout the life of the offspring. Thus NaCl passed from mothers to their offspring via milk until the pups were 20 days old. Some mice also consumed the NaCl diet directly as of about day 17.

Blood for measurement of serum CK activity and TA muscle for morphological analysis, as well as for determination of inorganic ion concentration and TA muscle fibers for metal elements, was collected from the same mouse. The number of mice used in this study is shown in the results. Our male and female B10, as well as mdx mice that were fed a standard diet (CE-2, Clea Japan), are able to produce offspring for 6 to 14 mo. Mouse experiments were performed in strict accordance with the guidelines of the National Institute of Neuroscience, National Center of Neurology and Psychiatry of Japan and were approved by the Animal Investigation Committee of the Institute.

Measurement of serum CK activity. The blood of mice (*day 7* to *90*) was withdrawn by inserting a syringe into the vena cava inferior of mice under deep ether anesthesia. The blood was then transferred to a 1.5-ml Eppendorf tube, allowed to stand for 2 h at room temperature, and centrifuged at 8,000 rpm using a TOMY MRX-150 centrifuge at

Address for reprint requests and other correspondence: Mizuko Yoshida, Department of Degenerative Neurological Disease, National Institute of Neuroscience, NCNP, 4-1-1 Ogawahigashi, Kodaira, Tokyo 187–8052, Japan (e-mail: yoshidam@ncnp.go.jp).

The costs of publication of this article were defrayed in part by the payment of page charges. The article must therefore be hereby marked "*advertisement*" in accordance with 18 U.S.C. Section 1734 solely to indicate this fact.

Table 1. *Mice serum creatine kinase (CK) activity, blood K^+ and Ca^{2+} concentration in male and female mdx and B10 mice from days 7 to 90*

Age, days	Strain	Sex	CK activity × 10^3, U/l	K^+, mM	Ca^{2+}, mM
7	mdx	M	0.360±0.122 (n=28)[a]		
		F	0.347±0.107 (n=29)[b]		
		M + F		3.9±0.29 (n=31)[a]	1.51±0.0387 (n=31)
	B10	M	0.355±0.160 (n=32)		
		F	0.397±0.178 (n=26)		
		M + F		3.8±0.30 (n=29)	1.54±0.0695 (n=29)
20	mdx	M	7.80±4.58 (n=33)[c]		
		F	7.86±4.31 (n=33)[d]		
		M + F		4.9±0.44 (n=28)[b]	1.31±0.0417 (n=28)
	B10	M	0.235±0.0598 (n=37)[e]		
		F	0.244±0.0442 (n=33)[f]		
		M + F		3.7±0.30 (n=29)	1.30±0.0363 (n=29)
60	mdx	M	15.3±13.1 (n=32)[g]		1.23±0.0431 (n=31)[a]
		F	6.73±3.97 (n=33)[h]		1.25±0.0330 (n=32)
		M + F		5.0±0.47 (n=56)[h]	
	B10	M	0.105±0.0771 (n=23)		1.20±0.0334 (n=30)[b]
		F	0.051±0.0145 (n=28)		1.23±0.0344 (n=31)[c]
		M + F		3.6±0.31 (n=60)	
90	mdx	M	16.8±10.1 (n=33)[i]		1.17±0.0334 (n=27)[d]
		F	7.91±4.97 (n=32)[j]		1.19±0.0353 (n=30)[e]
		M + F		5.0±0.61 (n=58)[h]	
	B10	M	0.084±0.0500 (n=34)		1.17±0.0243 (n=30)[f]
		F	0.065±0.0542 (n=34)		1.20±0.0280 (n=29)[g]
		M + F		3.6±0.32 (n=59)[c]	

Values are presented as means ± SD. Mice were fed a standard diet. M, male; F, female; n, number of mice examined. CK activity (serum): a vs. c, b vs. d, c vs. e, d vs. f, g vs. h, i vs. j, $P < 0.001$; c vs. g, $P < 0.004$. K^+ concentration: a vs. b, b vs. c, $P < 0.001$. Ca^{2+} concentration: a vs. b, $P < 0.002$; b vs. c, $P < 0.001$; d vs. e, $P < 0.01$; f vs. g, $P < 0.001$.

4°C (Tomy Seiko, Japan). Serum CK activity was determined with a Cica liquid CK test (Kanto Chemical, Japan) using Synchron CX7 (Beckman Coulter, Fullerton, CA).

Measurement of K^+, Ca^{2+}, and Na^+ concentrations in blood. Blood was collected into 1-ml syringes without anticoagulants by heart puncture under ether anesthesia. The blood was placed immediately in an i-STAT cartridge ($EC6^+$) (i-STAT, Princeton, NJ). The measurement of Ca^{2+}, Na^+, and K^+ concentrations was performed within 2.5 min after drawing blood.

Measurement of total potassium, calcium, sodium, magnesium, and zinc contents in muscle and food. The muscle was excised under deep ether anesthesia. TA muscle or food was placed in Teflon tubes and digested with 0.5 ml of ultrapure HNO_3 (Kanto Chemical) at 100°C for 2 h. The samples were diluted to 10 ml with ultrapure water. Potassium, calcium, sodium, magnesium, and zinc contents were determined using inductively coupled plasma emission spectrometry (P-4010, Hitachi High-Technologies, Tokyo, Japan).

Morphological analyses of TA muscle tissue. TA muscles of mice at *day 20* were excised and frozen immediately in isopentane cooled in liquid nitrogen. Cryostat transverse sections were stained by Carrazi's hematoxylin and eosin Y (1% solution; Muto Pure Chemical, Tokyo, Japan). Necrotic areas of muscle fibers were identified as described (6, 16) and analyzed with a Color Image Analyzer (SP-500 Olympus Optical, Tokyo, Japan). Necrotic areas correspond to the whole TA muscle area minus the white color area and normal (peripherally nucleated) fibers.

Statistics. Data are expressed as means ± SE or ± SD. The data were analyzed using the two-tailed Student's t-test.

RESULTS

Critical starting point of muscle fiber degeneration and differences between adult males and females. At the start of the study of the effect of NaCl on the degeneration of mdx muscle fibers, we decided to inhibit mdx muscle degeneration before the onset of muscle fiber necrosis. As shown in Table 1, the serum CK activity and blood K^+ concentration of mdx mice at *day 7* were similar to those of control B10 mice. Average serum CK activity and blood K^+ concentration in mdx mice began to increase only after *day 7*, and the K^+ concentration at *day 8* (*day 8*: 4.2 ± 0.1 mM, $P < 0.02$) and CK activity at *day 10* (*day 10*: 499 ± 28 U/l, $P < 0.001$) were significantly different from those at *day 7*. Serum CK activity and blood K^+ concentration also were significantly different for mdx mice between *days 7* and *20* ($P < 0.001$; Table 1). The results shown in Table 1 show that the serum CK activity and the K^+ concentration in blood of mdx mice began to increase after *day 7* compared with those of B10 mice, suggesting that the mdx cell membrane started to rupture after *day 7*, causing the CK and the K^+ to leak from muscle fibers to ECS. On the basis of these results, we started NaCl administration before *day 7*.

Blood Ca^{2+} concentration of both mdx and B10 female mice at *day 90* was significantly higher than that of males (Table 1). Although the differences of Ca^{2+} concentration between female and male mdx and B10 mice were small, the differences may be advantageous for the discussion, since blood Ca^{2+} concentration is strictly controlled (36). Serum CK activity of female mdx mice was about half of males' serum CK activity, as described in the introduction (Table 1). The values for serum CK activity in adult mdx mice are consistent with those reported by Suh et al. (38) and Takagi et al. (40).

Female TA muscle zinc contents of mdx and B10 mice were significantly higher than those in males of mdx and B10 mice. Muscle Zn content of mdx males was markedly higher than that of B10 males (Table 2).

Table 2. *Total zinc content in the tibialis anterior muscle of mdx and B10 male and female mice on day 60*

Sex	mdx	B10
M	13.7 ± 0.216^{a} ($n=30$)	12.2 ± 0.216^{c} ($n=30$)
F	14.8 ± 0.272^{b} ($n=28$)	15.7 ± 0.339^{d} ($n=30$)

Values are means ± SE. Zinc content is given in mg/kg wet weight. Mice were fed a standard diet. a vs. b, $P < 0.005$; c vs. d, a vs. c, $P < 0.001$; b vs. d, $P < 0.04$.

Effect of NaCl ingestion on serum CK activity and on morphology of mdx mice. We preliminarily examined whether a diet containing 1, 3, and 5% Na weight/weight (wt/wt) fed to mothers reduced serum CK activity of the offspring. Although 1 and 3% Na was insufficient, the diets containing 5% Na (In the following expression, a diet with 12% NaCl was used.) effectively reduced serum CK of mdx mice at *day 20* (Fig. 1). Therefore, these conditions were used in this study. The effect of NaCl ingestion on serum CK activity of mdx on *day 20* is shown in Fig. 1. The activity of this marker enzyme of muscle fiber degeneration was reduced to about 60% of that of mdx mice fed control food.

TA muscle fibers of mdx mice showed variations in fiber size, shape, and the incidence of large, dark fibers, and necrotic fibers were increased (Fig. 2, mdx). In contrast, the TA muscle fibers of mice whose mothers ate a diet with elevated NaCl were nearly normal in appearance (Fig. 2, mdx-Na). The area of necrosis in TA muscle sections from mdx-Na mice was drastically lowered (0.46% of total area, $n = 12$) compared with mdx mice (46%, $n = 17$) ($P < 0.001$). In addition, sections from the mdx-Na mice showed a nearly normal muscle pattern.

Effect of NaCl ingestion on blood K^+, Ca^{2+}, and Na^+ concentrations. The effect of NaCl ingestion (via mothers' milk) on blood K^+ and Ca^{2+} concentration of mdx-Na and control mice is shown in Fig. 3. Although NaCl had no effect on blood K^+ concentration in control mice, this ion was 11% lower in mdx-Na than in mdx mice ($P < 0.001$; Fig. 3*A*).

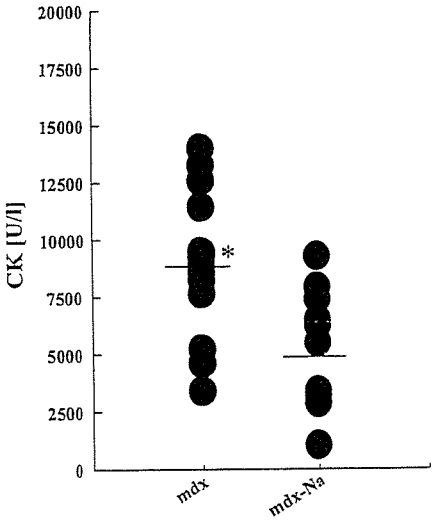

Fig. 1. Effect of NaCl ingestion on serum CK activity in mdx-Na mice at day 20. Mdx mice ($n = 16$) were fed a standard diet. Mdx-Na ($n = 13$) mice were fed a diet containing 12% NaCl (wt/wt); *$P < 0.001$. Horizontal lines indicate mean values.

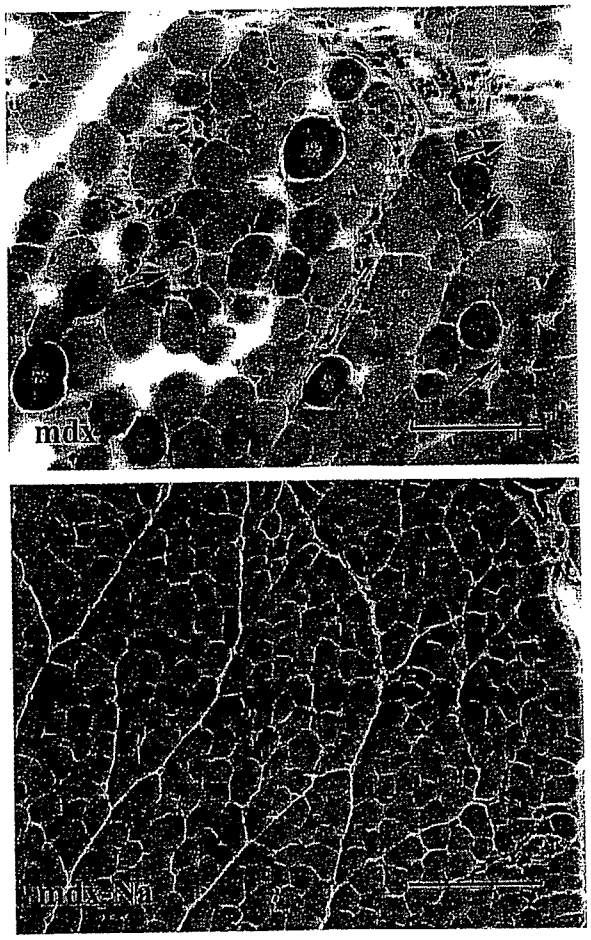

Fig. 2. Tibialis anterior muscle fibers from 20-day-old mdx mice fed a standard diet (mdx) and mdx-Na mice fed a diet containing 12% NaCl (mdx-Na). Muscle fibers from the mdx mouse show size variation, round shape, and large dark fibers (*), as well as necrotic fibers (arrows). Scale bars indicate 100 μm.

Blood Ca^{2+} and Na^+ levels in mdx-Na and control mice were significantly elevated compared with those on the control diet (Ca^{2+}: Fig. 3*B*, Na^+: data not shown).

Effect of NaCl ingestion on calcium, sodium, potassium, magnesium, and zinc content in TA muscle. The calcium and sodium content of TA muscles from mdx mice were markedly higher than those from B10 mice (Fig. 4, Ca and Na). NaCl administration significantly increased B10-Na muscle calcium ($P < 0.02$) and Na contents ($P < 0.001$). However, muscle calcium and sodium contents of mdx-Na mice were dramatically lower than those of mdx mice (both $P < 0.001$) and close to the levels in B10-Na mice.

Muscle potassium and magnesium contents in mdx mice were significantly lower compared with B10 mice (both $P < 0.001$; Fig. 4, K and Mg). In mdx-Na mice, muscle potassium and magnesium contents were noticeably higher as a result of NaCl supplementation (both $P < 0.001$).

The zinc content of muscle from mdx mice was significantly lower than that of the B10 controls ($P < 0.001$; Fig. 4, Zn). NaCl administration markedly elevated the muscle zinc content of both mdx-Na and B10-Na mice (both $P < 0.001$). Muscle Zn content of mdx-Na mice was close to that of B10 mice, but the difference was significant ($P < 0.01$).

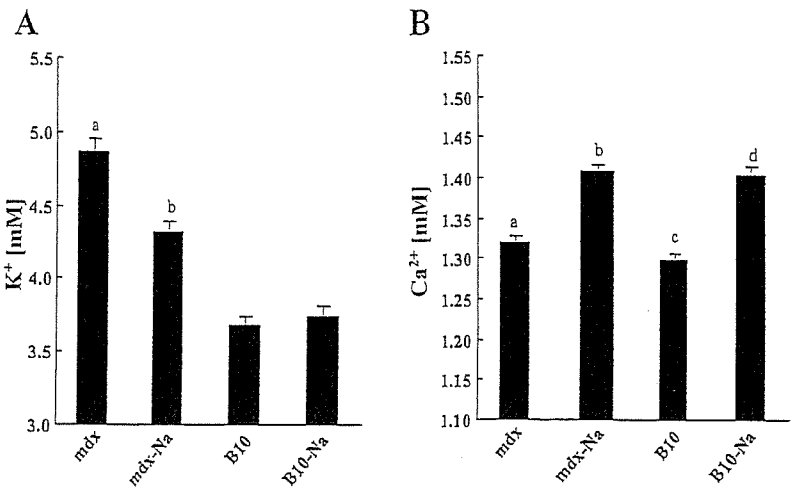

Fig. 3. Effect of NaCl ingestion on blood K^+ and Ca^{2+} concentration in mdx-Na and in B10-Na mice at day 20. *A:* K^+ concentration; mdx (n = 28) and B10 (n = 28) were fed a standard diet, mdx-Na (n = 29) and B10-Na (n = 29) were fed a diet containing 12% NaCl. a vs. b, $P < 0.001$. *B:* Ca^{2+} concentration; mdx (n = 27), mdx-Na (n = 28), B10 (n = 30), and B10-Na (n = 31), a vs. b, c vs. d, $P < 0.001$. Bars are mean, and vertical lines are SE.

DISCUSSION

We found earlier that mdx mice given saline by injection exhibited significantly reduced serum CK activity. We have now investigated whether oral supplementation of NaCl reduced serum CK activity and inhibited mdx muscle degeneration if given before the onset of muscle fiber necrosis.

Results in Table 1 show that the serum CK activity and the K^+ concentration in the blood of mdx mice began to increase after *day 7* compared with those of B10 mice, suggesting that the mdx cell membrane started to rupture after *day 7*, causing the CK and the K^+ to leak from muscle fibers into ECS. On the basis of these results, we started NaCl administration before *day 7*. NaCl-supplement administration significantly reduced muscle fiber degeneration of mdx mice at *day 20* (Figs. 1 and 2). NaCl administration also reduced blood K^+ concentration (Fig. 3*A*) and muscle sodium content (Fig. 4, Na), and increased potassium and magnesium in muscle fibers in mdx-Na mice (Fig. 4, K and Mg). The muscle calcium content of mdx-Na mice decreased drastically compared with that of mdx mice (Fig. 4, Ca) and close to the levels in B10-Na mice. The 99% decrease in the area of necrotic fibers in mdx-Na mice shows that NaCl supplementation almost completely inhibits mdx TA muscle fiber necrosis (Fig. 2). In mdx-Na and B10-Na mice, blood Na^+ and Ca^{2+} concentrations (Ca^{2+}: Fig. 3*B*) and muscle zinc content (Fig. 4, Zn) increased on *day 20* relative to the control. It is unknown why NaCl administration increased both zinc content in muscle fibers and blood Ca^{2+} concentration concurrently.

These results may have important implications for the inhibition of muscle necrosis, as Ca^{2+}, Na^+ and Zn^{2+} play critical physiological roles. We expect that the process of muscle degeneration in DMD or mdx mice causes excess Ca^{2+} to accumulate gradually in fibers after reaching a critical point in time, because their muscle fibers appear to function normally until a critical period is reached (47). In the case of mdx mice, the serum CK activity and K^+ concentration do not increase until around age 7 days (Table 1). When muscle fibers, with high levels of accumulated calcium, receive stimulation, the fibers subsequently undergo extreme hypercontraction at the critical point (after age 7 days) and may lead to membrane rupture (47). At this moment, K^+ may leak into the ECS and might produce the contraction of other muscle fibers around the ruptured fibers [potassium-induced contracture (27)].

We believe that group necrosis of muscle fibers following the efflux of K^+ may be one of the causes of necrosis of muscle fibers, in addition to the "theories on grouped necrosis" described by Gorospe et al. (20). The TA muscles of mdx-Na mice did not show group necrosis except in one case. Aside from the Ca^{2+}-stabilizing effect, reduced serum CK activity, blood K^+ concentration, and the group necrosis fibers of mdx-Na mice may have been caused by a quick, excessive K^+ excretion with excessive Na^+ excretion in urine, as the urinary potassium excretion rate depends on urinary volume (35). The mice that ingested the Na supplement drank excessive water and evacuated a large amount of urine, although we do not have data on the volume of their urine. Atrial natriuretic peptide (ANP) in the blood of the mice that ingested the Na supplement might have increased, since the high-salt diet induces an increase in ANP plasma levels (28). ANP has been also known to block sarcolemmal L-type Ca^{2+} channel activity and the Ca^{2+} release from the sarcoplasmic reticulum (SR) (25). The L-type Ca^{2+} channels and the Ca^{2+} release from the SR in mdx-Na muscle fibers may have been inhibited by the ANP, which prevents calcium accumulation in mdx-Na muscle fibers.

Mouse skeletal muscle fibers possess a Na^+/Ca^{2+} exchange mechanism (1). High Na^+ levels in the ECS serve to force efflux of Ca^{2+} from fibers via the Ca^{2+}/Na^+ exchanger and inhibit Ca^{2+} release from the SR (13). The average blood Na^+ concentration in mdx-Na and B10-Na mice was significantly elevated. Thus the Na^+/Ca^{2+} exchanger of mdx-Na muscle fibers may have prevented calcium accumulation in mdx-Na muscle fibers and might contribute to increase Ca^{2+} concentration in blood (and ECS).

Lijnen and Petrov (26) demonstrated reduction of the total calcium content of erythrocytes and the intraplatelet Ca^{2+} concentration by calcium supplementation. The mean value of serum Ca^{2+} concentration and the plasma total calcium content of the treated calcium group was higher than in the placebo group, although there are no significant differences between the calcium and placebo groups. They also showed a reduction in the plasma concentrations of intact parathormone and 1,25-dihydroxyvitamin D3 that raise calcium uptake in cells (7, 9). Increased Ca^{2+} concentration in the blood of mdx-Na might have been produced to reduce the activity of parathormone and

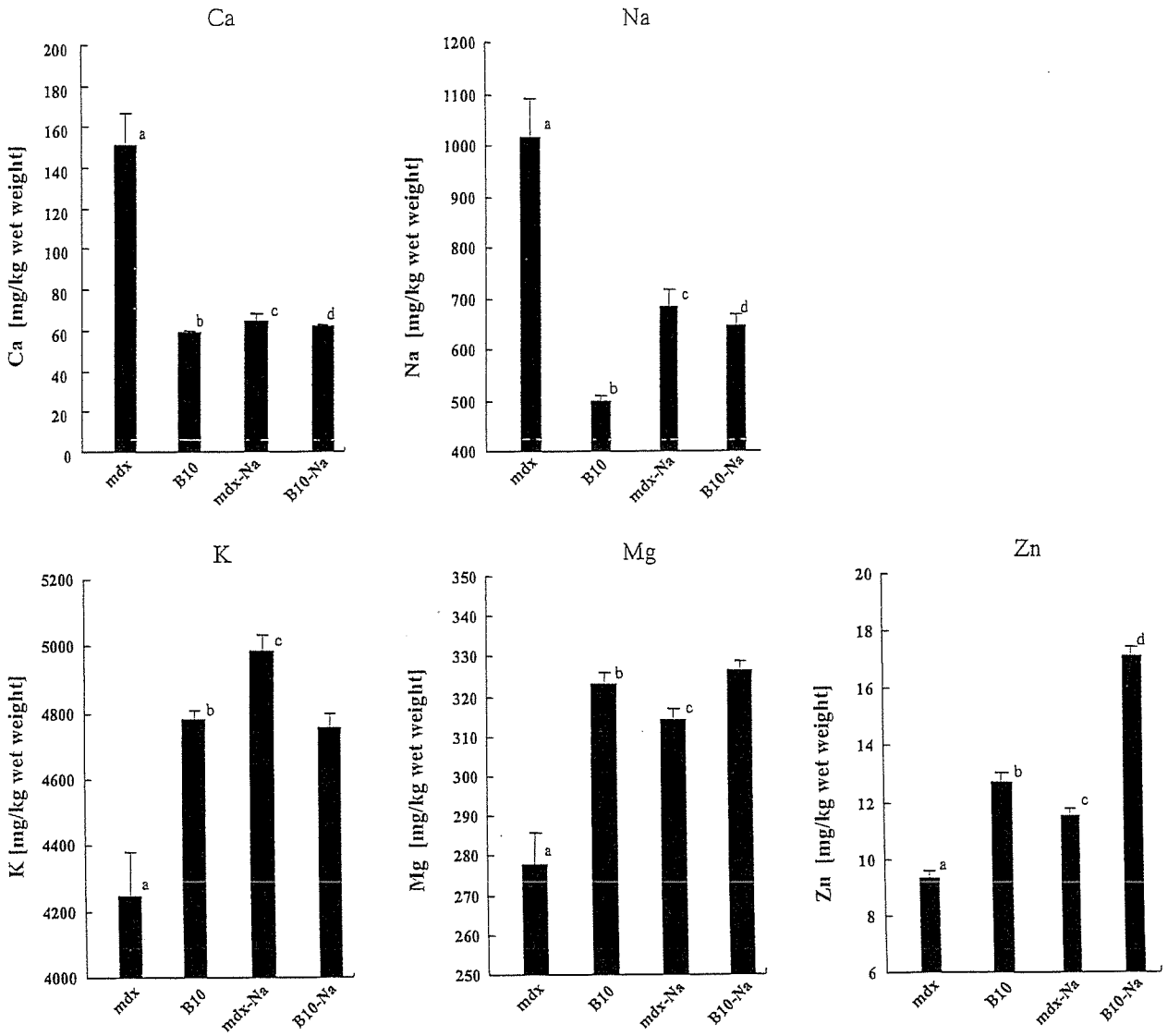

Fig. 4. Effect of NaCl ingestion on total calcium, sodium, potassium, magnesium, and zinc content in the tibialis anterior muscle of mdx-Na and B10-Na mice at *day 20*. Mdx and B10 were fed a standard diet; mdx-Na and B10-Na were fed a diet containing 12% NaCl. Ca, calcium content; mdx (n = 29), B10 (n = 31), mdx-Na (n = 25) and B10-Na (n = 27); a vs. b, a vs. c, $P < 0.001$; b vs. d, $P < 0.02$. Na: sodium content; mdx (n = 29), B10 (n = 31), mdx-Na (n = 25), and B10-Na (n = 27); a vs. b, a vs. c, b vs. d, $P < 0.001$. K: potassium content: mdx (n = 30), B10 (n = 31), mdx-Na (n = 25) and B10-Na (n = 27). a vs. b, a vs. c, $P < 0.001$. Mg: magnesium content; mdx (n = 29), B10 (n = 31), mdx-Na (n = 25) and B10-Na (n = 30); a vs. b, a vs. c, $P < 0.001$. Zn: zinc content; mdx (n = 30) and B10 (n = 31), mdx-Na (n = 27) and B10-Na (n = 30); a vs. b, a vs. c, b vs. d, $P < 0.001$. Bars are means, and vertical lines are SE.

1,25-dihydroxyvitamin D3 and may have prevented calcium accumulation in muscle fibers of mdx mice.

Activation of Ca^{2+}-ATPase of erythrocytes by calcium supplementation (49) and high activity of Ca^{2+}-ATPase in dystrophic muscle sarcolemma (14, 39) were demonstrated. High Ca^{2+} concentration in the blood of mdx-Na mice may have induced Ca^{2+}-ATPase to higher activity for the prevention of Ca^{2+} accumulation in muscle fibers and might have protected them from calcium accumulation in muscle fibers of mdx mice. From the above discussions, it is conceivable that higher Ca^{2+} in the blood (or in ECS) of female mdx mice reduced the calcium accumulation in their muscle fibers, inhibited necrosis of muscle fibers, and stabilized membrane effects of Ca^{2+}.

The zinc content of TA muscle of mdx-Na or female mdx mice was higher than that of muscle of mdx mice fed a control diet or of male mdx mice. Zinc may be important to inhibit muscle necrosis because Zn^{2+} stabilizes cell membranes (5) and blocks L-type Ca^{2+} channels (45). One of the reasons why serum CK activity in mdx females is lower than in males may be higher zinc content of muscle than that of muscle of males. Muscle zinc content of mdx males was markedly higher than that of B10 males (Table 2). These results suggest the importance of zinc in mdx mice surviving as long as control B10 mice. Mdx males seem to require higher muscle zinc content to survive as long as B10 mice. Zn^{2+} also plays a role in protein synthesis and may contribute to the regeneration of muscle fibers. Therefore, Zn^{2+} may be important for muscle regeneration in mdx mice. The assumption is supported by the results of Tameyasu et al. (41), which suggest that the administration of a zinc compound ameliorates muscle function in the mdx

mouse. The standard feed used in this study and in the Laboratory Animal Facility of the National Institute of Neuroscience, NCNP, contains approximately two times the calcium, six times the potassium, six times the magnesium, seven times the sodium, and six times the zinc as the estimated minimal mineral requirements for mice (31). Hence, the mice in this study and at our institute may have ingested necessary calcium, sodium, and zinc in their diet to survive as long as B10 mice.

Our results suggest that blood Ca^{2+} concentration, muscle zinc content, and potassium excretion are important for the inhibition of muscle fiber necrosis in mdx mice.

In future studies, we will further investigate the cause-and-effect relationship of NaCl supplementation to identify effective therapies for reducing the rate of muscle degeneration and improving the quality of life of DMD patients.

ACKNOWLEDGMENTS

We give grateful thanks to Drs. O. Imazawa, A. Ishii, I. Kamo, and A. Takahashi [National Center of Neurology and Psychiatry (NCNP)], as well as M. Date (Riken) for helpful support and discussions; to S. Wakai (NCNP) for assistance measuring serum CK activity and to Prof. W. L. Stahl (University of Washington, Seattle) and Dr. I. Nonaka (NCNP) for critically reading the manuscript. Special thanks are also given to Prof. U. T. Ruegg (University of Geneva) for critical discussions, suggestions, and reading.

GRANTS

This work was supported in part by a grant-in-aid from the NCNP of the Ministry of Health, Labour and Welfare of Japan.

REFERENCES

1. **Balnave CD and Allen DG.** Evidence for Na+/Ca^{2+} exchange in intact single skeletal muscle fibers from the mouse. *Am J Physiol Cell Physiol* 274: C940–C946, 1998.
2. **Beam KG.** Duchenne muscular dystrophy. Localizing the gene product. *Nature* 333: 798–799, 1988.
3. **Bertorini TE, Bhattacharya SK, Palmieri GM, Chesney CM, Pifer D, and Baker B.** Muscle calcium and magnesium content in Duchenne muscular dystrophy. *Neurology* 32: 1088–1092, 1982.
4. **Bertorini TE, Cornelio F, Bhattacharya SK, Palmieri GM, Dones I, Dworzak F, Brambati B, Chesney CM, Pifer D, and Baker B.** Calcium and magnesium content in fetuses at risk and prenecrotic Duchenne muscular dystrophy. Muscle calcium and magnesium content in Duchenne muscular dystrophy. *Neurology* 34: 1436–1440, 1984.
5. **Bettger WJ and O'Dell BL.** Physiological roles of zinc in the plasma membrane of mammalian cells. *J Nutr Biochem* 4: 194–207, 1993.
6. **Bodensteiner JB and Engel AG.** Intracellular calcium accumulation in Duchenne dystrophy and other myopathies: a study of 567,000 muscle fibers in 114 biopsies. *Neurology* 28: 439–446, 1978.
7. **Bogin E, Massry SG, Levi J, Djaldeti M, Bristol G, and Smith J.** Effect of parathyroid hormone on osmotic fragility of human erythrocytes. *J Clin Invest* 69: 1017–1025, 1982.
8. **Buetler TM, Renard M, Offord EA, Schneider H, and Ruegg UT.** Green tea extract decreases muscle necrosis in mdx mice and protects against reactive oxygen species. *Am J Clin Nutr* 75: 749–753, 2002.
9. **Bukoski RD, Xue H, and McCarron DA.** Effect of 1.25(OH)2 vitamin D3 and ionized Ca2+ on 45Ca uptake by primary cultures of aortic myocytes of spontaneously hypertensive and Wistar-Kyoto normotensive rats. *Biochem Biophys Res Commun* 146: 1330–1335, 1987.
10. **Campbell KP and Kahl SD.** Association of dystrophin and an integral membrane glycoprotein. *Nature* 338: 259–262, 1989.
11. **Carpenter S and Karpati G.** Duchenne muscular dystrophy: plasma membrane loss initiates muscle cell necrosis unless it is repaired. *Brain* 102: 147–161, 1979.
12. **Collet C, Csernoch L, and Jacquemond V.** Intramembrane charge movement and L-type calcium current in skeletal muscle fibers isolated from control and mdx mice. *Biophys J* 84: 251–265, 2003.
13. **Deval E, Levitsky DO, Marchand E, Cantereau A, Raymond G, and Cognard C.** Na(+)/Ca(2+) exchange in human myotubes: intracellular calcium rises in response to external sodium depletion are enhanced in DMD. *Neuromuscul Disord* 12: 665–673, 2002.
14. **Dhalla NS, McNamara DB, Balasubramanian V, Greenlaw R, and Tucker FR.** Alterations of adenosine triphosphatase activities in dystrophic muscle sarcolemma. *Res Commun Chem Pathol Pharmacol* 6: 643–650, 1973.
15. **Emery AE.** Population frequencies of inherited neuromuscular diseases—a world survey. *Neuromuscul Disord* 1: 19–29, 1991.
16. **Engel AG, Yamamoto M, and Fischbeck KH.** Dystrophinopathies. In: *Myology* (2nd ed.), edited by Engel AG and Franzini-Armstrong, C. New York: McGraw-Hill, 1133–1187, 1994.
17. **Fisher I, Abraham D, Bouri K, Hoffman EP, Muntoni F, and Morgan J.** Prednisolone-induced changes in dystrophic skeletal muscle. *FASEB J* 19: 834–836, 2005.
18. **Fong PY, Turner PR, Denetclaw WF, and Steinhardt RA.** Increased activity of calcium leak channels in myotubes of Duchenne human and mdx mouse origin. *Science* 250: 673–676, 1990.
19. **Glesby MJ, Rosenmann E, Nylen EG, and Wrogemann K.** Serum CK, calcium, magnesium, and oxidative phosphorylation in mdx mouse muscular dystrophy. *Muscle Nerve* 11: 852–856, 1988.
20. **Gorospe JRM, Nishikawa BK, and Hoffman EP.** Pathophysiology of dystrophin deficiency: a clinical and biological enigma. In: *Dystrophin Gene, Protein and Cell Biology*, edited by Brown SC and Lucy JA; New York: Cambridge University Press, pp. 201–232, 1997.
21. **Goyenvalle A, Vulin A, Fougerousse F, Leturcq F, Kaplan JC, Garcia L, and Danos O.** Rescue of dystrophic muscle through U7 snRNA-mediated exon skipping. *Science* 306: 1796–1799, 2004.
22. **Harper SQ, Hauser MA, DelloRusso C, Duan D, Crawford RW, Phelps SF, Harper HA, Robinson AS, Engelhardt JF, Brooks SV, and Chamberlain JS.** Modular flexibility of dystrophin: implications for gene therapy of Duchenne muscular dystrophy. *Nat Med* 8: 253–261, 2002.
23. **Hubner C, Lehr HA, Bodlaj R, Finckh B, Oexle K, Marklund SL, Freudenberg K, Kontush A, Speer A, Terwolbeck K, Voit T, and Kohlschutter A.** Wheat kernel ingestion protects from progression of muscle weakness in mdx mice, an animal model of Duchenne muscular dystrophy. *Pediatr Res* 40: 444–449, 1996.
24. **Jackson MJ, Jones DA, and Edwards RH.** Measurements of calcium and other elements in muscle biopsy samples from patients with Duchenne muscular dystrophy. *Clin Chim Acta* 147: 215–221, 1985.
25. **Jin JY, Wen JF, Li D, and Cho KW.** Osmoregulation of atrial myocytic ANP release: osmotransduction via cross-talk between L-type Ca^{2+} channel and SR Ca^{2+} release. *Am J Physiol Regul Integr Comp Physiol* 287: R1101–R1109, 2004.
26. **Lijnen P and Petrov V.** Dietary calcium, blood pressure and cell membrane cation transport systems in males. *J Hypertens* 13: 875–882, 1995.
27. **Luttgau HC.** The action of calcium ions on potassium contractures of single muscle fibres. *J Physiol* 168: 679–697, 1963.
28. **Marchi Alves LM, Tosi LR, Antunes-Rodrigues J, and Carnio EC.** Is there a link between salt-intake and atrial natriuretic peptide system during hypertension induced by nitric oxide blockade? *Regul Pept* 120: 127–132, 2004.
29. **Maunder-Sewry CA, Gorodetsky R, Yarom R, and Dubowitz V.** Element analysis of skeletal muscle in Duchenne muscular dystrophy using x-ray fluorescence spectrometry. *Muscle Nerve* 3: 502–508, 1980.
30. **McArdle A, Edwards RH, and Jackson MJ.** Accumulation of calcium by normal and dystrophin-deficient mouse muscle during contractile activity in vitro. *Clin Sci (Lond)* 82: 455–459, 1992.
31. **National Research Council.** Nutrient requirements of the mouse. In: *Nutrient Requirements of Laboratory Animals*, Washington, D.C.: National Academy Press, chapt. 3, p. 80, 1995.
32. **Okinaka S, Kumagai H, Ebashi S, Sugita H, Momoi H, Toyokura Y, and Fujie Y.** Serum creatine phosphokinase. Activity in progressive muscular dystrophy and neuromuscular diseases. *Arch Neurol* 4: 520–525, 1961.
33. **Passaquin AC, Renard M, Kay L, Challet C, Mokhtarian A, Wallimann T, and Ruegg UT.** Creatine supplementation reduces skeletal muscle degeneration and enhances mitochondrial function in mdx mice. *Neuromuscul Disord* 12: 174–182, 2002.
34. **Reeve JL, McArdle A, and Jackson MJ.** Age-related changes in muscle calcium content in dystrophin-deficient mdx mice. *Muscle Nerve* 20: 357–360, 1997.

35. **Reineck HJ, Osgood RW, Ferris TF, and Stein JH.** Potassium transport in the distal tubule and collecting duct of the rat. *Am J Physiol* 229: 1403–1409, 1975.
36. **Shiramine K, Aou S, and Hori T.** Lateral hypothalamic injection of GABA(A) antagonist induces gastric vagus-mediated hypocalcemia in the rat. *Am J Physiol Regul Integr Comp Physiol* 273: R1492–R1500, 1997.
37. **Spencer MJ and Mellgren RL.** Overexpression of a calpastatin transgene in mdx muscle reduces dystrophic pathology. *Hum Mol Genet* 11: 2645–2655, 2002.
38. **Suh JG, Yamazaki A, and Tomita T.** Breeding of the gad-mdx mouse: influence of genetically induced denervation on dystrophic muscle fibers. *Lab Anim Sci* 44: 42–46, 1994.
39. **Sulakhe PV, Fedelesova M, McNamara DB, and Dhalla NS.** Isolation of skeletal muscle membrane fragments containing active Na+-K+ stimulated ATPase: comparison of normal and dystrophic muscle sarcolemma. *Biochem Biophys Res Commun* 42: 793–800, 1971.
40. **Takagi A, Watanabe T, Kojima S, and Endo Y.** Effect of long-term administration of prednisolone on serum creatine kinase and muscle pathology of mdx mouse. *Rinsho Shinkeigaku* 38: 724–728, 1998.
41. **Tameyasu T, Yamada M, Tanaka M, and Takahashi S.** Effect of zinc-carnosine chelate compound on muscle function in mdx mouse. *Jpn J Physiol* 52: 111–120, 2002.
42. **Tinsley JM, Potter AC, Phelps SR, Fisher R, Trickett JI, and Davies KE.** Amelioration of the dystrophic phenotype of mdx mice using a truncated utrophin transgene. *Nature* 384: 349–353, 1996.
43. **Wang Z, Zhu T, Qiao C, Zhou L, Wang B, Zhang J, Chen C, Li J, and Xiao X.** Adeno-associated virus serotype 8 efficiently delivers genes to muscle and heart. *Nat Biotechnol* 23: 321–328, 2005.
44. **Watkins SC, Hoffman EP, Slayter HS, and Kunkel LM.** Immunoelectron microscopic localization of dystrophin in myofibres. *Nature* 333: 863–866, 1988.
45. **Winegar BD and Lansman JB.** Voltage-dependent block by zinc of single calcium channels in mouse myotubes. *J Physiol* 425: 563–578, 1990.
46. **Yilmaz O, Karaduman A, and Topaloglu H.** Prednisolone therapy in Duchenne muscular dystrophy prolongs ambulation and prevents scoliosis. *Eur J Neurol* 11: 541–544, 2004.
47. **Yoshida M, Matsuzaki T, Date M, and Wada K.** Skeletal muscle fiber degeneration in mdx mice induced by electrical stimulation. *Muscle Nerve* 20: 1422–1432, 1997.
48. **Zatz M, Shapiro LJ, Campion DS, Oda E, and Kaback MM.** Serum pyruvate-kinase (PK) and creatine-phosphokinase (CPK) in progressive muscular dystrophies. *J Neurol Sci* 36: 349–362, 1978.
49. **Zemel MB, Bedford BA, Zemel PC, Marwah O, and Sowers JR.** Altered cation transport in non-insulin-dependent diabetic hypertension: effects of dietary calcium. *J Hypertens Suppl* 6: S228–S230, 1988.

OPEN ACCESS Freely available online

Identification of Mitochondrial DNA Polymorphisms That Alter Mitochondrial Matrix pH and Intracellular Calcium Dynamics

An-a Kazuno[1,2☯], Kae Munakata[1☯], Takeharu Nagai[3,4¤], Satoshi Shimozono[3], Masashi Tanaka[5], Makoto Yoneda[6], Nobumasa Kato[2], Atsushi Miyawaki[3], Tadafumi Kato[1*]

1 Laboratory for Molecular Dynamics of Mental Disorders, Brain Science Institute, RIKEN, Saitama, Japan, 2 Department of Neuropsychiatry, Faculty of Medicine, University of Tokyo, Tokyo, Japan, 3 Laboratory for Cell Function and Dynamics, Brain Science Institute, RIKEN, Saitama, Japan, 4 Structure and Function of Biomolecules, Precursory Research for Embryonic Science and Technology, Japan Science and Technology Agency, Saitama, Japan, 5 Genomics for Longevity and Health, Tokyo Metropolitan Institute of Gerontology, Tokyo, Japan, 6 Second Department of Internal Medicine, University of Fukui Faculty of Medical Sciences, Fukui, Japan

Mitochondrial DNA (mtDNA) is highly polymorphic, and its variations in humans may contribute to individual differences in function as well as susceptibility to various diseases such as Parkinson disease, Alzheimer disease, bipolar disorder, and cancer. However, it is unclear whether and how mtDNA polymorphisms affect intracellular function, such as calcium signaling or pH regulation. Here we searched for mtDNA polymorphisms that have intracellular functional significance using transmitochondrial hybrid cells (cybrids) carrying ratiometric Pericam (RP), a fluorescent calcium indicator, targeted to the mitochondria and nucleus. By analyzing the entire mtDNA sequence in 35 cybrid lines, we found that two closely linked nonsynonymous polymorphisms, *8701A* and *10398A*, increased the basal fluorescence ratio of mitochondria-targeted RP. Mitochondrial matrix pH was lower in the cybrids with *8701A/10398A* than it was in those with *8701G/10398G*, suggesting that the difference observed by RP was mainly caused by alterations in mitochondrial calcium levels. Cytosolic calcium response to histamine also tended to be higher in the cybrids with *8701A/10398A*. It has previously been reported that *10398A* is associated with an increased risk of Parkinson disease, Alzheimer disease, bipolar disorder, and cancer, whereas *10398G* associates with longevity. Our findings suggest that these mtDNA polymorphisms may play a role in the pathophysiology of these complex diseases by affecting mitochondrial matrix pH and intracellular calcium dynamics.

Citation: Kazuno A, Munakata K, Nagai T, Shimozono S, Tanaka M, et al. (2006) Identification of mitochondrial DNA polymorphisms that alter mitochondrial matrix pH and intracellular calcium dynamics. PLoS Genet 2(8): e128. DOI: 10.1371/journal.pgen.0020128

Introduction

The central importance of mitochondria in ATP production is well established [1,2]. The pH gradient across the mitochondrial membrane and the inner mitochondrial membrane potential make up the electrochemical gradient, which regulates the efficiency of ATP synthesis and other mitochondrial activity. Recent studies are also focusing on the roles of mitochondria in regulation of intracellular calcium dynamics. Mitochondrial calcium uptake affects various important cellular processes such as apoptosis [3–5], exocytosis [6,7], synaptic plasticity [8], and possibly spine dynamics [9].

Mitochondria have their own DNA, mitochondrial DNA (mtDNA), which encodes the genes of 22 transfer RNAs (tRNAs), 2 ribosomal RNAs (rRNAs), and 13 subunits of enzymes related to oxidative phosphorylation [10]. Other subunits of mitochondrial proteins are encoded in the nuclear genome.

Mutations in mtDNA are known to cause various mitochondrial diseases such as mitochondrial myopathy, encephalopathy, lactic acidosis, and stroke-like episodes (MELAS), which is caused by the *3243A/G* mutation in mtDNA [11,12]. The mechanisms by which these mtDNA mutations cause functional impairment are well studied [13,14]. On the other hand, mtDNA is highly polymorphic, and certain polymorphisms are thought to be risk factors in complex diseases such as diabetes mellitus [15], Alzheimer disease [16,17], Parkinson disease [18–21], bipolar disorder [22,23], and some kinds of cancer [24,25]. It has also been reported that mtDNA polymorphisms are related to interindividual functional variability in human cognition [26], personality [27], athletic performance [28], and longevity [29]. However, these associations are solely dependent on population genetics. It is difficult to draw a definite conclusion from genetic association analyses alone because the high variability of mtDNA

Editor: Harry Orr, University of Minnesota, United States of America

Received June 17, 2005; **Accepted** June 28, 2006; **Published** August 11, 2006

DOI: 10.1371/journal.pgen.0020128

Abbreviations: cybrid, transmitochondrial hybrid cell; mt DsRed, mitochondria-targeted red fluorescent protein from *Discosoma*; mt pH-GFP, mitochondria-targeted pH-sensitive green fluorescent protein; mtDNA, mitochondrial DNA; mtRP, ratiometric Pericam targeted to mitochondria; mtSNPs, mitochondrial DNA single nucleotide polymorphisms; nucRP, ratiometric Pericam targeted to nucleus; RP, ratiometric Pericam; rRNA, ribosomal RNA; tRNA, transfer RNA

* To whom correspondence should be addressed. E-mail: kato@brain.riken.jp

☯ These authors contributed equally to this work.

¤ Current address: Laboratory of Nanosystems Physiology, Research Institute for Electronic Science, Hokkaido University, Hokkaido, Japan

Synopsis

Mitochondria play important roles in energy production and regulation of intracellular calcium levels. Mitochondria have their own genetic material, mitochondrial DNA (mtDNA). In spite of its short length (16.6 kbp), mtDNA is highly variable among individuals and is thought to contribute to interindividual functional variability in energy-requiring activities such as intelligence and athletic performance. However, it is unclear whether mtDNA polymorphisms affect intracellular function and condition. Using transmitochondrial hybrid cells, the authors found two closely linked mtDNA polymorphisms—*10398A/G* and *8701A/G*—which cause alterations in mitochondrial pH and calcium concentration. Cytosolic calcium response to histamine tended to be different between transmitochondrial hybrid cells carrying these two mtDNA polymorphisms. It has been reported that the *10398A* mtDNA polymorphism is a risk factor for Parkinson disease, Alzheimer disease, cancer, and bipolar disorder, whereas *10398G* is associated with longevity. The present findings suggest that these mtDNA polymorphisms may play a role in the pathophysiology of these complex diseases by affecting mitochondrial matrix pH and intracellular calcium dynamics.

among individuals makes such analysis susceptible to confounding effects of population stratification; in addition, the effects of other polymorphisms in mitochondrial or nuclear genes are difficult to control. Although functional analyses of these polymorphisms are needed, to date there are few reports that identify functional effects of mtDNA polymorphisms. This is mainly due to methodological difficulties, as conventional molecular biological techniques are not readily applicable to mtDNA.

We examined the phenotypic effect of mitochondrial DNA without interference from nuclear genes by analysing transmitochondrial hybrid cells (cybrids), which were made by fusing a cell line lacking mtDNA, called ρ^0 (rho zero) cells [30], with platelets from humans. Although the consequences of pathogenic mtDNA mutations have been examined using this technique, the functional significance of mtDNA polymorphisms has not been well investigated yet.

In this study, we searched for functional mtDNA polymorphisms using the following strategies: (1) by targeting a calcium indicator, ratiometric Pericam (RP) [31], to mitochondria and the nucleus in the same cell, mitochondrial and cytosolic calcium levels were monitored simultaneously; (2) to reduce cellular variability, a ρ^0 cell line was subcloned before generation of cybrids; (3) by sequencing the whole mtDNA genome in 35 cybrids, functional mtDNA polymorphisms were comprehensively analyzed, and two nonsynonymous mtDNA polymorphisms, *10398A/G* and *8701A/G*, were identified; and (4) using a pH indicator, we confirmed that these mtDNA polymorphisms altered both mitochondrial matrix pH and intracellular calcium levels.

Results

Generation and Confirmation of Cybrid Cell Lines

First, we established a 143B.TK$^-$ $\rho^0$206 cell line that stably expresses two RPs. RP is a ratiometric fluorescent protein developed as a calcium indicator [31]. The fluorescence ratio of 510 nm emission at 480 nm excitation to that at 410 nm excitation is reported to reflect calcium concentration at a constant pH. Mitochondria-targeted RP is also sensitive to pH because there is a higher pH [32,33] in the mitochondrial matrix (approximately 7.7–8.0) [34,35] than in the cytosol. In this study, two RPs, one targeted to mitochondria (mtRP) and the other to the nucleus (nucRP), were expressed in the same living cell. Thus, we were able to simultaneously monitor mitochondrial and cytosolic calcium concentrations [31]. Because calcium levels in the nucleus were reported to be similar to those in cytosol, nuclear calcium levels were used to indicate cytosolic calcium level.

We subcloned several ρ^0 cell lines carrying RPs and selected one that showed a reproducible calcium response. We confirmed by mtDNA-specific PCR and Southern blot analysis that this cell line lacked mtDNA. We fused this cell line with platelets taken from 35 human volunteers and confirmed the integration of mtDNA from the volunteers by Southern blot analysis.

Measurements of Fluorescence Ratio of mtRP in all Cybrid Cell Lines

Using these cybrids, we measured fluorescence ratios of mtRP and nucRP. In fluorescent images of cybrids, mitochondria had a higher 480 nm/410 nm ratio than the nucleus (Figure 1A), possibly reflecting higher calcium levels and pH in mitochondrial matrix than in cytosol. This result is consistent with previous observations in HeLa cells [32]. At first, baseline fluorescence ratios were recorded for 2 minutes. Subsequently, cells were stimulated by 10 μM histamine, which elicits inositol trisphosphate–mediated calcium release from the endoplasmic reticulum [36]. In the first 60 s following stimulation, the fluorescence ratio of mtRP and nucRP initially increased and then returned to basal levels (Figure 1B). The mtRP fluorescence ratio was measured in 11–42 cells for each of the 35 cell lines by fluorescent microscopy.

Using a one-way analysis of variance, we tested whether or not interindividual variation of mtDNA causes differences in basal mtRP fluorescence ratios. A statistically significant variation of basal mtRP fluorescence ratios was found among these cybrid lines ($p < 0.001$, $F = 6.328$).

Entire Sequences of mtDNA in All Cybrid Cell Lines

To identify the mtDNA polymorphisms that cause heterogeneity among cybrids, we determined the entire 16.5-kbp sequence of mtDNA in each of the 35 cybrids. mtDNA polymorphisms were selected in comparison with the revised Cambridge Reference Sequence [10,37]. A total of 216 polymorphic sites, including 13 novel polymorphisms, were identified. All cybrids had different sequences.

Identification of mtDNA Polymorphisms Altering the Fluorescence Ratio of mtRP

To identify the polymorphisms with functional significance, all nonsynonymous polymorphisms or polymorphisms in tRNA or rRNA found in more than three cybrids ($n = 16$) were selected (Table 1). For each polymorphism, the average mtRP fluorescence ratios for two genotypes at the particular polymorphic site were compared (Table 1). The polymorphisms at only two positions, 8701 and 10398, showed nominally significant differences of basal mtRP fluorescence ratios. Basal mtRP fluorescence ratios in cybrids with mtDNA *10398A* were significantly higher than those with *10398G*

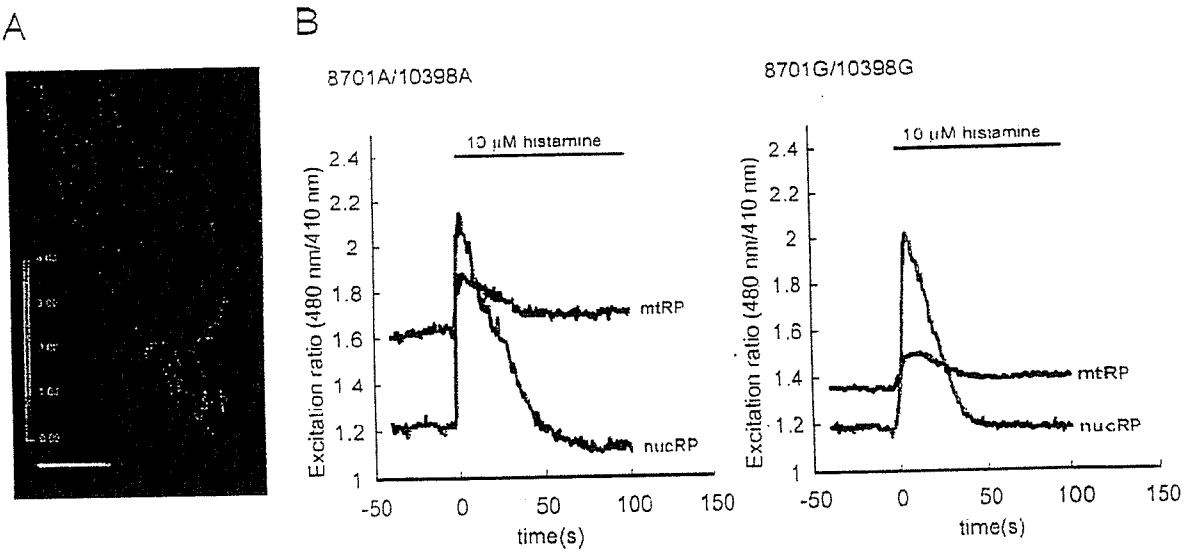

Figure 1. Typical Excitation Ratio Image of a Cybrid and Histograms Showing Responses to Histamine

(A) Image of a typical cybrid showing fluorescence ratios of excitation at 480 nm to 410 nm in pseudocolors. Mitochondria had a higher 480 nm/410 nm ratio than the nucleus, possibly reflecting higher calcium levels and pH in mitochondrial matrix than in cytosol. Scale bar, 10 μm.

(B) Representative fluorescence ratio responses of *8701A/10398A* cybrids (left) and *8701G/10398G* cybrids (right) evoked by 10 μM histamine. The *y* axis shows the ratio of the 525 nm fluorescence at 480 nm to that at 410 nm. Blue traces show the ratio in the nucleus and red traces show the ratio in mitochondria. Histamine (10 μM) was added at time 0 s and was not washed out during the experiment.

DOI: 10.1371/journal.pgen.0020128.g001

(*10398A*, 1.67 ± 0.09 [mean ± SD], $n = 11$; *10398G*, 1.59 ± 0.12 [mean ± SD], $n = 24$; $p < 0.05$, Mann-Whitney *U* test). Basal mtRP fluorescence ratios in the cybrids with *8701A* were also significantly higher than those with *8701G* (*8701A*, 1.67 ± 0.1 [mean ± SD], $n = 18$; *8701G*, 1.59 ± 0.11 [mean ± SD], $n = 22$; $p < 0.05$). Because *8701A* was linked to *10398A* in all but two cybrids, it was difficult to assess the independent effects of these polymorphisms. Since these two cybrids showed intermediate values (average fluorescence ratio, 1.64), it suggests that both of these polymorphisms may contribute to the observed difference. Because there were only two subjects with *8701G/10398A*, further analyses were performed using only *8701A/10398A* and *8701G/10398G* cybrids.

Basal mtRP fluorescence ratios in cybrids with *8701A/10398A* mtDNA were significantly higher than those with *8701G/10398G* mtDNA (*8701A/10398A*, 1.67 ± 0.09 [mean ± SD], $n = 11$; *8701G/10398G*, 1.59 ± 0.11 [mean ± SD], $n = 22$; $p < 0.05$, Mann-Whitney *U* test; Figures 1 and 2). Peak mtRP fluorescence ratios after the histamine stimulation also showed a similar but nonsignificant trend (*8701A/10398A*, 1.86 ± 0.11 [mean ± SD]; *8701G/10398G*, 1.78 ± 0.14 [mean ± SD]; $p = 0.05$).

Replication Study Using Cybrid Cell Lines Stably Expressing RP

Because the nominally significant effects of polymorphisms at positions 10398 and 8701 on basal mtRP fluorescence ratio were found after multiple statistical analyses, we performed a second study to ensure it was not a false-positive finding. Three cybrid lines with *8701A/10398A* mtDNA and three with *8701G/10398G* mtDNA were chosen from among the 35 cybrids for the replication study (Table S1). The results confirmed our initial observation of a higher basal mtRP fluorescence ratio in cybrids with mtDNA *8701A/10398A* (*8701A/10398A*, 1.78 ± 0.04 [mean ± SD], three cell lines; *8701G/10398G*, 1.67 ± 0.01 [mean ± SD], three cell lines). Peak mtRP fluorescence ratios after the histamine stimulation also showed a similar trend (*8701A/10398A*, 1.99 ± 0.04 [mean ± SD], three cell lines; *8701G/10398G*, 1.88 ± 0.02 [mean ± SD], three cell lines).

Replication Study Using Independently Established Cybrid Cell Lines

To further confirm that the observed difference is caused by the difference of mtDNA sequence, we performed another replication study using independently established cybrid cell lines. In this experiment, the native 143B.TK$^-$ $\rho^0$206 cell line was used without any further subcloning. We established independent cybrid cell lines by using platelets derived from a subgroup of the original 35 donors (Table S1). By transiently transfecting the cybrids with *ratiometric coxIV-Pericam* cDNA, fluorescence imaging was performed. Moreover, cells were stimulated by 10 μM histamine, and in vivo calibration was performed using calibration buffers with ionomycin, which equilibrate intramitochondrial and extracellular calcium. To minimize the cell-to-cell variability, an index for calcium level, $(R - R_{min}) / (R_{max} - R)$ (see Materials and Methods), was analyzed in cells responded to histamine. As a result, our initial observation in cybrids with mtDNA *8701A/10398A* was confirmed (*8701A/10398A*, 1.07 ± 0.40 [mean ± SD], three cell lines; *8701G/10398G*, 0.51 ± 0.09 [mean ± SD], three cell lines; Figure S1).

Generation of pH Indicator for Measurements of Mitochondrial Matrix pH

It has been reported that the fluorescence ratio of RP is dependent not only on calcium levels but also on pH [32,33].

Table 1. The mtDNA Polymorphisms in 35 Cybrids

Nucleotide Change	Gene[a]	Amino Acid Change[b]	Number of Subjects[c]		Basal Fluorescence Ratio of Mitochondria-Targeted RP[f]		Statistical Analysis[g]	Disease Related[h]
			Anderson Sequence[d]	Non-Anderson Sequence[e]	Anderson Sequence	Non-Anderson Sequence	*p*	
A633T	tRNA Pro		34	1	—	—	—	
A663G	12S rRNA		31	4	1.61	1.70	0.213	
G709A	12S rRNA		30	5	1.63	1.58	0.962	
A750G	12S rRNA		0	35	—	—	—	
C752T	12S rRNA		34	1	—	—	—	
A827G	12S rRNA		32	3	1.62	1.65	—	
C922T[i]	12S rRNA		34	1	—	—	—	
T1107C	12S rRNA		34	1	—	—	—	
C1310T	12S rRNA		33	2	—	—	—	DM
A1382C	12S rRNA		34	1	—	—	—	
T1413C	12S rRNA		34	1	—	—	—	
A1438G	12S rRNA		1	34	—	—	—	DM
G1442A	12S rRNA		34	1	—	—	—	
T1452C	12S rRNA		34	1	—	—	—	
G1598A	12S rRNA		34	1	—	—	—	
A1736G	16S rRNA		31	4	1.61	1.70	0.213	
A2109T[i]	16S rRNA		34	1	—	—	—	
T2150-51TA[j]	16S rRNA		31	4	1.61	1.70	0.213	
T2404C	16S rRNA		34	1	—	—	—	
T2626C	16S rRNA		30	5	1.62	1.59	0.480	
A2706G	16S rRNA		1	34	—	—	—	
C2766T	16S rRNA		34	1	—	—	—	
C2772T	16S rRNA		30	5	1.62	1.59	0.480	
G2831A	16S rRNA		34	1	—	—	—	
G3010A	16S rRNA		24	11	1.62	1.62	0.749	
C3204T	16S rRNA		34	1	—	—	—	
C3206T	16S rRNA		32	3	1.62	1.65	—	
G3391A	ND1	G29S	34	1	—	—	—	
A3434G	ND1	Y43C	34	1	—	—	—	
T3644C	ND1	V113A	34	1	—	—	—	
G4048A	ND1	D248N	33	2	—	—	—	
T4386C	tRNA Gln		30	5	1.62	1.59	0.480	
A4824G	ND2	T119A	31	4	1.61	1.70	0.213	
A4833G	ND2	T122A	32	3	1.63	1.46	—	
C5178A	ND2	L237M	23	12	1.62	1.62	0.677	
C5263T	ND2	A265V	34	1	—	—	—	
A5301G	ND2	I278V	34	1	—	—	—	
T5418C	ND2	F317L	33	2	—	—	—	
G5460A	ND2	A331T	32	3	1.63	1.48	—	AD, PD
G5773A	tRNA Cys		33	2	—	—	—	
A6040G	COI	N46S	34	1	—	—	—	
C6318T[i]	COI	P139S	34	1	—	—	—	
G7269A[i]	COI	V456M	34	1	—	—	—	
T7270C	COI	V456A	34	1	—	—	—	
T7297C[i]	COI	V465A	34	1	—	—	—	
G7444A	COI	Ter514K	34	1	—	—	—	LHON, SNHL
G7521A	tRNA Asp		34	1	—	—	—	
G7664A	COII	A27T	34	1	—	—	—	
A7673G	COII	T30V	34	1	—	—	—	
G7853A	COII	V90I	33	2	—	—	—	
G7859A	COII	D92N	34	1	—	—	—	
C8414T	ATP8	L17F	24	11	1.62	1.62	0.749	
A8563G	ATP6	T13A	31	4	1.61	1.70	0.213	
G8584A	ATP6	A20T	34	1	—	—	—	
A8701G	ATP6	T59A	13	22	1.67	1.59	**0.037**	
G8764A	ATP6	A80T	34	1	—	—	—	
C8794T	ATP6	H90Y	31	4	1.61	1.70	0.213	
A8860G	ATP6	T112A	0	35	—	—	—	
C9011T[i]	ATP6	A162V	34	1	—	—	—	
A9355G	COIII	N50S	34	1	—	—	—	
G9477A	COIII	V91I	34	1	—	—	—	
A9670G	COIII	N155S	34	1	—	—	—	
T10345C	ND3	I96T	33	2	—	—	—	
A10398G	ND3	T114A	11	24	1.67	1.59	**0.036**	
T10410C	tRNA Arg		32	3	1.62	1.65	—	

Table 1. Continued

Nucleotide Change	Gene[a]	Amino Acid Change[b]	Number of Subjects[c]		Basal Fluorescence Ratio of Mitochondria-Targeted RP[f]		Statistical Analysis[g]	Disease Related[h]
			Anderson Sequence[d]	Non-Anderson Sequence[e]	Anderson Sequence	Non-Anderson Sequence	*p*	
G10427A	tRNA Arg		34	1	—	—	—	
G11016A	ND4	S86N	34	1	—	—	—	
A11084G	ND4	T109A	30	5	1.62	1.59	0.480	MELAS
T11255C	ND4	Y166H	34	1	—	—	—	
A12026G	ND4	I423V	34	1	—	—	—	DM
C12135T	ND4	S459F	33	2	—	—	—	
G12236A	tRNA Ser		34	1	—	—	—	
A12358G	ND5	T8A	32	3	1.62	1.65	—	
A12361G	ND5	T9A	34	1	—	—	—	
T12811C	ND5	Y159H	33	2	—	—	—	
T12880C	ND5	F182L	33	2	—	—	—	
A13651G	ND5	T439A	34	1	—	—	—	
G13928A	ND5	S531N	34	1	—	—	—	
A13942G	ND5	T536A	33	2	—	—	—	
A14053G	ND5	T573A	34	1	—	—	—	
T14178C	ND6	I166V	34	1	—	—	—	
A14693G	tRNA Glu		34	1	—	—	—	
A14696G	tRNA Glu		34	1	—	—	—	
C14766T	Cytb	T7I	0	35	—	—	—	
G14858A	Cytb	G38S	34	1	—	—	—	
T14979C	Cytb	I78T	32	3	1.62	1.65	—	
A15218G	Cytb	T158A	34	1	—	—	—	
A15236G	Cytb	I164V	34	1	—	—	—	
G15314A	Cytb	A190T	34	1	—	—	—	
G15323A	Cytb	A193T	33	2	—	—	—	
A15326G	Cytb	T194A	0	35	—	—	—	
C15468T[i]	Cytb	T241M	34	1	—	—	—	
T15479C	Cytb	F245L	34	1	—	—	—	PIEI
G15497A	Cytb	G251S	33	2	—	—	—	
A15662G	Cytb	I306V	34	1	—	—	—	
A15758G	Cytb	T338V	34	1	—	—	—	
A15851G	Cytb	I369V	34	1	—	—	—	
A15860G	Cytb	I372V	33	2	—	—	—	
A15901G[i]	tRNA Thr		34	1	—	—	—	
G15927A	tRNA Thr		34	1	—	—	—	
G15930A	tRNA Thr		33	2	—	—	—	
T15940C	tRNA Thr		34	1	—	—	—	
G16000A	tRNA Pro		34	1	—	—	—	

Boldface entries, $p < 0.05$.

[a]ND1, ND2, ND3, ND4, ND5, ND6, genes encoding subunits of complex I (NADH dehydrogenase); COI, COII, COIII, subunits of complex IV (cytochrome c oxidase); ATP8, ATP6, subunits of complex V (ATP synthase); and Cytb, a subunit of complex III (ubiquinol: cytochrome c oxidoreductase).

[b]For example, G29S means that the G3391A causes substitution from glycine (G) to serine (S) at the 29th amino acid of the ND1 gene.

[c]The number of subjects among 35 cybrids.

[d]The revised Cambridge Reference Sequence.

[e]Only the bases that differed from Anderson sequence are shown.

[f]Each value indicates the excitation ratio (480 nm/410 nm).

[g]Mann-Whitney *U* test was applied only when the number of subjects in both groups were larger than three.

[h]The polymorphisms denoted as "disease related" in the MITOMAP database, a human mitochondrial genome database (http://www.mitomap.org).

[i]Polymorphisms newly identified in this study.

[j]Insertion.

AD, Alzheimer disease; DM, diabetes mellitus; LHON, Leber hereditary optic neuropathy; MELAS, mitochondrial encephalomyopathy, lactic acidosis, and stroke-like episodes; SNHL, sensorineuronal hearing loss; PIEI, paracrystalline inclusions with exercise intolerance.

DOI: 10.1371/journal.pgen.0020128.t001

especially at the higher pH range found in the mitochondrial matrix. To test the relative contributions of these factors to the observed finding, we attempted to measure mitochondrial pH using mitochondria-targeted, pH-sensitive green fluorescent protein (mt pH-GFP) [38,39] and mitochondria-targeted red fluorescent protein from *Discosoma* (mt DsRed) expressed under the control of a bidirectional promoter [40–42]. Because the pKa of pH-GFP is approximately 8.0, it is useful for measuring mitochondrial matrix pH. Since DsRed is a pH-insensitive protein, it can be used as a reference [43].

We confirmed that this pH indicator, mt pH-GFP/DsRed, could be successfully used to measure mitochondrial pH.

Measurements of Mitochondrial Matrix pH in Cybrids with mtDNA *8701A/10398A* and *8701G/10398G*

For the measurements of mitochondrial matrix pH, we used the above-mentioned independently established lines of

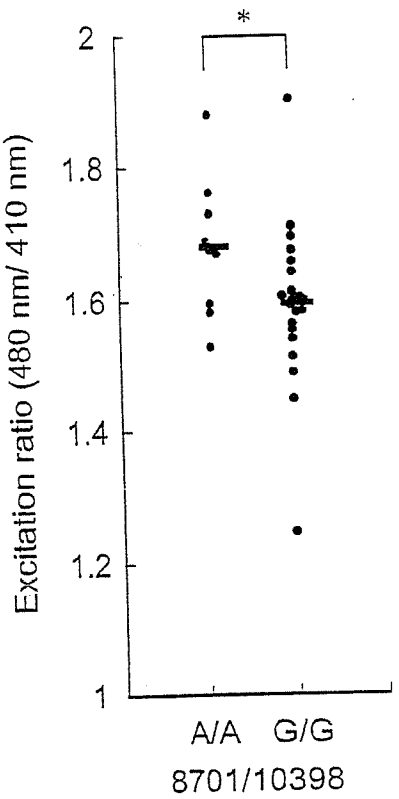

Figure 2. Effects of *10398A/G* on Basal Fluorescence Ratios of Mitochondria-Targeted RP

Differences between the basal fluorescence ratios in *10398A* and *10398G* cybrids are shown. All cybrids with *8701A* have *10398A* (left). While most cybrids with *8701G* had *10398G* (right), two cybrids had *8701A* and *10398G* (the data of these two cybrids were 1.52 and 1.77). For each cybrid, data taken from 11–42 cells (average, 26 cells) were averaged. The *y* axis shows the ratio of the 525 nm fluorescence at 480 nm to that at 410 nm. Horizontal bars indicate the mean values for each type of cybrid. $^*p < 0.05$ (Mann-Whitney *U* test).

DOI: 10.1371/journal.pgen.0020128.g002

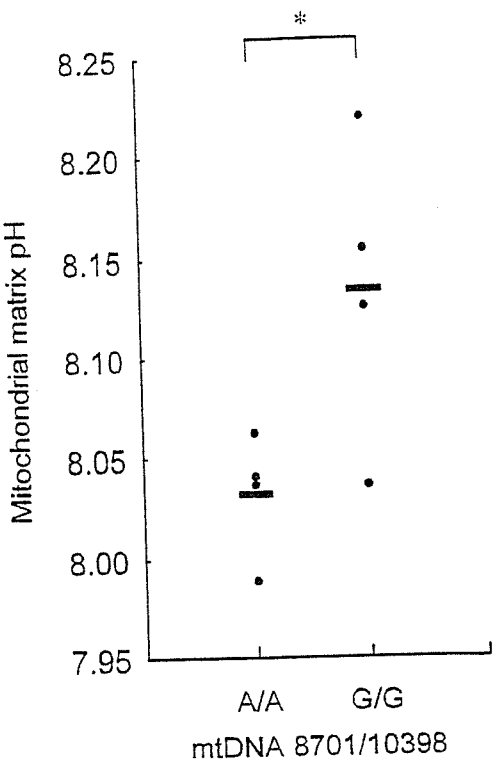

Figure 3. Basal Mitochondrial Matrix pH in the Cybrids with *8701A/10398A* or *8701G/10398G*

Data from 11–18 cells in a triplicate experiment were averaged for each of four cell lines in each group. The *y* axis shows mitochondrial matrix pH calculated by calibration in vivo. Horizontal bars indicate the mean values for each type of cybrid. $^*p < 0.05$ (*t* test).

DOI: 10.1371/journal.pgen.0020128.g003

cybrids generated from the native 143B.TK$^-$ ρ^0 206 cell line that does not carry RPs (four with *8701A/10398A* and four with *8701G/10398G*). By transiently cotransfecting the mt pH-GFP/DsRed and Tet-Off vectors, basal mitochondrial matrix pH was recorded for several minutes in each cybrid cell line. We performed in vivo calibration of mitochondrial basal matrix pH in each cell by using four calibration buffers (pH 7.0, 7.5, 8.0, and 8.5) with the ionophores nigericin and monensin, which equilibrate intramitochondrial and extracellular pH. The calculated basal mitochondrial matrix pH was about 8.0, which is consistent with previous reports using HeLa cells and ECV304 cells [34,35]. Compared with the *8701G/10398G* cybrids, the basal mitochondrial matrix pH was significantly lower in the *8701A/10398A* cybrids (*8701A/10398A*, 8.03 ± 0.03 [mean ± SD], four cell lines; *8701G/10398G*, 8.13 ± 0.07 [mean ± SD], four cell lines; $p < 0.05$, *t* test; Figure 3).

Cytosolic Calcium Dynamics

To test whether or not these mtDNA polymorphisms affect cytosolic calcium dynamics, we examined the effects of *8701A/10398A* and *8701G/10398G* genotypes on the cytosolic calcium levels.

The nucRP data from the first experiments indicated that the *8701A/10398A* cybrids tended to have higher peak cytosolic calcium levels after the histamine stimulation compared with the *8701G/10398G* cybrids (*8701A/10398A*, 2.10 ± 0.14 [mean ± SD], 11 cell lines; *8701G/10398G*, 2.02 ± 0.15, 22 cell lines, [mean ± SD]; $p = 0.08$, Mann-Whitney *U* test; Figure 4). There was no significant difference of basal cytosolic calcium level (*8701A/10398A*, 1.29 ± 0.07 [mean ± SD], 11 cell lines; *8701G/10398G*, 1.25 ± 0.07 [mean ± SD], 22 cell lines; $p > 0.10$, Mann-Whitney *U* test). This result suggests that cytosolic calcium response may be enhanced in the *8701A/10398A* cybrids.

The nucRP data from the replication study using cybrid cell lines stably expressing RP confirmed that peak cytosolic calcium levels after histamine stimulation were higher in the *8701A/10398A* cybrids than in *8701G/10398G* cybrids (*8701A/10398A*, 2.56 ± 0.03 [mean ± SD], three cell lines; *8701G/10398G*, 2.26 ± 0.16 [mean ± SD], three cell lines).

Discussion

In the present study, we comprehensively searched for mtDNA polymorphisms that alter the fluorescence ratios of mtRP, and we identified two mtDNA single nucleotide

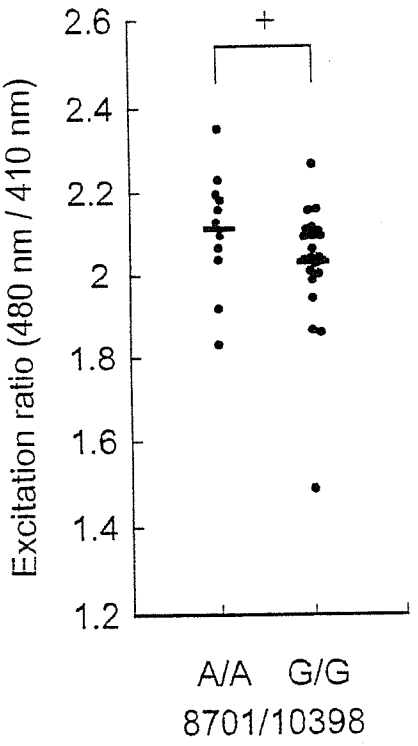

Figure 4. Peak Cytosolic Calcium Level after Histamine Stimulation in Cybrids with *8701A/10398A* and *8701G/10398G*

The values of two cybrids with *8701A/10398G* were 1.92 and 2.20. For each cybrid, data taken from 11–42 cells (average, 26 cells) were averaged. The *y* axis shows the ratio of the 525 nm fluorescence at 480 nm to that at 410 nm. Horizontal bars indicate the mean values for each type of cybrid. +$p = 0.08$ (Mann-Whitney *U* test).

DOI: 10.1371/journal.pgen.0020128.g004

polymorphisms (mtSNPs), *10398A* and *8701A*, that increase the basal fluorescence ratios of mtRP.

In the *10398A/G* mtSNP, threonine is substituted by alanine at the C terminus of ND3, a subunit of complex I (NADH: ubiquinone oxidoreductase) [10]. In the *8701A/G* mtSNP, there is an amino acid substitution from threonine to alanine at ATPase6, the F0 subunit 6 of complex V (ATP synthase) [10]. Complex I generates a proton gradient across mitochondrial inner membrane by exporting protons, whereas ATP synthase produces ATP by using this proton gradient. The proton gradient is also the driving force of calcium uptake by mitochondria. Therefore, both polymorphisms can affect the proton gradient across mitochondrial inner membrane and calcium levels.

During the course of our study, it was reported that the fluorescence ratio of RP is dependent not only on calcium levels but also on pH at the higher pH ranges in mitochondrial matrix [32,33]. Thus, we measured basal mitochondrial matrix pH in cybrids with *8701A/10398A* and *8701G/10398G*. Basal mitochondrial matrix pH was significantly lower in cybrids with *8701A/10398A* than in those with *8701G/10398G*. Alteration in mitochondrial pH has also been hypothesized to modulate ATP production, apoptosis, and the opening of the mitochondrial membrane permeability transition pore [44]. Transport of protons is coupled with electron transport by a respiratory chain consisting of complexes I, III, and IV. As described above, the mtDNA 10398 polymorphism affects the amino acid composition in a subunit of complex I. When the activity of complex I in the electron-transport chain was measured using citrate synthase activity as a reference [45], the activity of *8701A/10398A* cybrids tended to be lower than that of *8701G/10398G* cybrids (*8701A/10398A*, 5.77 ± 1.41 [mean ± SD], four cell lines; *8701G/10398G*, 7.58 ± 1.27 [mean ± SD], four cell lines; $p = 0.10$, *t* test). This finding supports the above-mentioned difference in mitochondrial matrix pH.

The difference in basal mitochondrial matrix pH could not contribute to the initial finding of higher mtRP fluorescence ratio in the cybrids with *8701A/10398A* because lower pH could only decrease the mtRP fluorescence rate, not increase it. Therefore, the most probable interpretation for the difference in basal mtRP fluorescence ratio is higher mitochondrial calcium levels in cybrids carrying *8701A/10398A*. In addition, the calcium responses to histamine stimulation tended to be higher in the cytosol of *8701A/10398A* cybrids than *8701G/10398G* cybrids, both in the initial experiment and the replication study using cybrid cell lines stably expressing RP. These findings suggest that alterations in mitochondrial function cause the enhanced cytosolic calcium response and higher basal mitochondrial calcium levels in cybrids with *8701A/10398A*.

Mitochondria have several calcium transport mechanisms. Calcium uptake is attributable to a mitochondrial calcium uniporter in inner mitochondrial membrane. Calcium efflux from mitochondria is mediated by the Na^+/Ca^{2+} exchanger and the H^+/Ca^{2+} antiporter. The opening of the membrane permeability transition pore also allows efflux of calcium from mitochondria. Clarification of mitochondrial calcium transport systems at the molecular level would facilitate the understanding of biochemical mechanism of how the 10398 polymorphism alters mitochondrial calcium dynamics. Further study is needed to reveal how these two mtSNPs alter mitochondrial matrix pH and calcium levels.

Among the two polymorphisms we found to have functional significance, *10398A/G* has previously been associated with human health and diseases. The *10398G* polymorphism is reportedly associated with a reduced risk of Parkinson disease [19], whereas *10398A* was reported to increase the risk of Alzheimer disease in men [17], invasive breast cancer in African-American women [24], and prostate cancer in African-American men [25]. In addition, *10398A* is reportedly associated with an increased risk of bipolar disorder [22,23,46]. According to the mtSNP database (http://www.gen-info.osaka-u.ac.jp/mitosnp/index_e.html), most Europeans have *8701A*, but it is polymorphic in the Japanese population. In contrast, *10398A* is polymorphic both in Europeans and Japanese. The *10398A/G* characterizes the European haplogroup I, J, and K [17], and Asian-specific super haplogroup M [47]. Thus, the present findings can be translated that Asian-specific super haplogroup M is associated with different mitochondrial pH and calcium from other Asian-specific haplogroups.

The frequency of *10398A* is much smaller in the Japanese population (approximately 29% in the mtSNP database) compared with Europeans (approximately 74% in the mtSNP database). The average life expectancy in Japan is the highest in the world, and its biological basis is not yet well understood. Tanaka et al. sequenced the whole mtDNA sequence in

11 Japanese centenarians and reported that a subset of haplogroup M characterized by several mtDNA polymorphisms is more frequently seen in centenarians [48]. Among these polymorphisms, they have mainly focused on the *5178A* polymorphism that characterizes haplogroup D in super haplogroup M. The *5178C/A* is associated with several common diseases such as Parkinson disease [28], atherosclerosis in patients with diabetes mellitus [49], and myocardial infarction [50]. A recent study, however, suggested that association of *5178A* with longevity is ethnicity dependent [51]. Therefore, it might be possible that these apparent effects of *5178C/A* in the Japanese population may be mediated by the other linked polymorphisms that cause functional change. Although *5178A* did not affect the fluorescence ratio of mtRP in this study, most subjects with *5178A* have *10398G*. Thus, it could be possible that *10398G* mediates these apparent associations of *5178C/A* with complex diseases and longevity. In fact, based on the mtSNP database, *10398G* was significantly more frequently seen in centenarians (76 of 96 [79%]) compared with young Japanese (129 of 192 [67%]; $p = 0.03$). A recent study by Niemi et al. also suggested that *10398G* affects longevity [52].

To date, there has been no study on the association of *8701A/G* with health and disease, and information on *8701A/G* is limited. Most of the above-noted associations with the 5178 polymorphism observed in the Japanese population could also be mediated by 8701, since it is closely linked with 10398 and 5178. In fact, *8701G* is also more frequency seen in centenarians (68 of 96 [71%]) compared with young Japanese (111 of 192 [58%]; $p = 0.03$).

It was difficult to assess the functional effects of these two mtSNPs separately, because there were only two subjects carrying *8701A/10398G* in our sample set. Although it is still an open question whether or not *8701A/G* causes some functional change, at least *10398A/G* seems to have some functional significance. The tendency of altered complex I activity between the *8701A/10398A* and *8701G/10398G* cybrids suggest that the observed difference between *8701A/10398A* and *8701G/10398G* is mediated at least partly by the functional alteration of complex I by *10398A/G*.

Because there was considerable overlap, including an outlier, with regard to the basal mtRP fluorescence between *8701A/10398A* and *8701G/10398G*, there might be a concern that the observed difference may be caused by those outliers. Thus, we applied the Smirnow-Grubbs test for the detection of outliers. One cell line, having the lowest value in the *8701G/10398G* group, was found to be an outlier ($T = 3.17$; $p < 0.05$). Even after this cell line was omitted, basal mtRP fluorescence ratios in cybrids with *8701A/10398A* were significantly higher than those with *8701G/10398G* (*8701A/10398A*, 1.67 ± 0.09 [mean ± SD], $n = 11$; *8701G/10398G*, 1.60 ± 0.09 [mean ± SD], $n = 21$; $p < 0.05$, Mann-Whitney *U* test). Thus, the observed difference was not due to the effect of the outlier. One might suspect that observed variation of basal mtRP fluorescence ratios might not be caused by mtDNA sequence variation but resulted from an experimental variation. However, the interassay variance within one cybrid cell line having the same mtDNA sequence was significantly smaller than the variation among cybrid cell lines having different mtDNA sequences. This indicates that observed variation of mtRP fluorescence ratios among cybrid cell lines were not caused by experimental variation but caused by the difference of mtDNA sequence.

There might be the other concern that the present finding is somehow affected by the process of subcloning, and such a finding cannot be generalized. However, in our replication study using independently established cybrid cell lines, it was confirmed that the observed finding was not specific to this particular subcloned cybrids, but was actually caused by differences of mtDNA sequences.

In summary, we identified two mtSNPs that were suggested to alter mitochondrial matrix pH and intracellular calcium dynamics. To our knowledge, this is the first report of mtDNA polymorphisms affecting these intracellular functions. Among the two mtSNPs examined, the *10398A/G* polymorphism was previously reported to be associated with Parkinson disease, Alzheimer disease, some kinds of cancer, bipolar disorder, and longevity. A drug that affects mitochondrial matrix pH or calcium levels might be a promising strategy for health and disease.

Materials and Methods

Subjects. Cybrids were generated from platelets derived from 35 volunteers, 17 patients with bipolar disorder (mean age, 48 years; 9 men and 8 women) and 18 healthy controls (mean age, 48 years; 10 men and 8 women). All were Japanese. Patients with bipolar disorder were included in this study because these blood samples were collected as a part of a project to study the genetics of bipolar disorder. None of the experimental parameters reported in this paper showed a significant difference between patients and controls. Diagnoses were made by the consensus of two senior psychiatrists using the DSM-IV criteria. Written informed consent was obtained from all volunteers. The Ethics Committees of the RIKEN Brain Science Institute and other participating institutes approved the study. For the replication study using cybrid cell lines stably expressing RP, we selected cybrids from three subjects with *8701A/10398A* mtDNA (mean age, 48 years; 1 man and 2 women) and three subjects with *8701G/10398G* mtDNA (mean age, 51 years; 1 man and 2 women). Cybrids for replication studies using independently established cybrid cell lines and measurements of mitochondrial matrix pH were generated using platelets from four *8701A/10398A* subjects (mean age, 52 years; 2 men and 2 women) and four *8701G/10398G* subjects (mean age, 56 years; 2 men and 2 women). Cybrids for replication studies and the measurement of mitochondrial matrix pH were derived from healthy controls. Although these cell lines have several mtDNA polymorphisms in addition to 8701 and 10398, they were carefully selected so that they have minimum difference in other positions of mtDNA.

Generation of the 143B.TK$^-$ $\rho^0$206 cell line stably carrying calcium-sensitive probes. The 143B.TK$^-$ $\rho^0$206 cell line derived from the osteosarcoma cell line (143B.TK$^-$) was established by Attardi and King [30]. The 143B.TK$^-$ $\rho^0$206 cells were grown in DMEM (Invitrogen, Carlsbad, California, United States), supplemented with 10% FBS, 50 U penicillin, 50 μg/ml streptomycin, and 50 μg/ml uridine. The cells were grown on dishes 35 mm in diameter to 50% confluence. The cells were cotransfected with Lipofect AMINE PLUS (Invitrogen) with *ratiometric Pericam-nuc* (0.25 μg DNA/dish) and *ratiometric coxIV-Pericam* (0.75 μg DNA/dish) cDNAs. After 2 d, these cells were replated onto coverslips 14 mm in diameter and allowed to grow to 2.5% confluence with selection medium, supplemented with 10% FBS, 1,000 μg/ml geneticin (Invitrogen), and 50 μg/ml uridine. After 2 wk, a single colony with fluorescence in nuclei and mitochondria was picked up under a fluorescent microscope. mtDNA-specific PCR and Southern blot analysis were used to confirm that the cells lacked mtDNA. The cell lines were replated onto coverslips and stimulated by histamine (Sigma-Aldrich, Saint Louis, Missouri, United States) as described below. One of the ten cell lines had a reproducible calcium response without spontaneous calcium oscillation. This line was selected for further examination.

Generation of cybrid cell lines. Peripheral blood was drawn into a 10 ml Vactainer tube containing 1.5 ml acid citrate dextrose (BD Biosciences, Palo Alto, California, United States). Platelets were separated by centrifugation at a speed of 1,200 rpm for 20 min. The

143B.TK⁻ ρ⁰206 cells that had been stably expressing RPs were fused with platelets from individuals using a polyethylene glycol solution [53]. After 3 d of fusion, the medium was replaced by a selection medium without uridine. After 2 wk, surviving cells were collected. The integration of mtDNA was verified by Southern blot analysis as previously described with some modifications [54]. Cybrids for the replication study using independently established cybrid cell lines and measurements of mitochondrial matrix pH were generated by fusing the native 143B.TK⁻ ρ⁰206 cells and platelets from individuals as described above.

Measurements of fluorescence ratios of RP. Cybrids in modified Krebs R buffer (125 mM NaCl, 5 mM KCl, 5.5 mM glucose, 20 mM HEPES, and 1 mM $MgCl_2$ [pH 7.4]) were imaged at room temperature on an Olympus IX-70 (Olympus, Tokyo, Japan) with a CoolSNAPHQ CCD camera (Roper Scientific, Tucson, Arizona, United States) controlled by Universal Imaging Meta series 4.5/4.6 (Universal Imaging, Media, Pennsylvania, United States). Dual-excitation imaging with RP used two excitation filters (480DF10 and 410DF10), alternated by a Lambda 10-2 filter exchanger (Sutter Instruments, Novato, California, United States), a 505DRLP-XR dichroic mirror, and a 525AF45 emission filter. The cybrids were stimulated by bath-application of 10 μM histamine applied to the coverslip. The ratio of the 525 nm fluorescence at 480 nm to that at 410 nm was used for further analysis. The regions of interest for measuring calcium response in each cell were the mitochondria and nucleus.

For each cell line, 11–42 cells were measured. At first, the basal fluorescence ratios of mtRP obtained from each cell were used for statistical analysis by one-way analysis of variance. Using one-way analysis of variance ($df = 34$), we tested whether or not the variation among 35 cybrid cell lines having different mtDNA was larger than the variation within one cell line. Then, the 11–42 data points in each cell line were averaged to calculate the representative value for each cell line.

The coefficient of variation in fluorescence ratio of mtRP in each cell line was 12.2% ± 3.2% (mean ± SD in 35 cybrids).

For the replication study using eight independently established cybrid cell lines (four with *8701A/10398A* mtDNA and four with *8701G/10398G* mtDNA), cybrids were transiently transfected with *ratiometric coxIV-Pericam* (1 μg DNA/dish) cDNA using Lipofect AMINE PLUS. After 2 d, measurements were performed in these cell lines. Different from the case in the cells stably expressing RP, there is no assurance that the expression level of RP is constant across cells in this experiment, which may potentially affect the stability of fluorescence ratio. To avoid the effect of variability of expression levels of RP among cells, we performed in vivo calibration for each cell. To exactly estimate calcium levels, we applied histamine stimulation to the cells, and only those responded to histamine were further analyzed. Cells responded to calcium could be found in three of four cell lines for each group. Cells were stimulated by 10 μM histamine, and calibration was performed using calibration buffers. Calcium-free buffer consisted of modified Krebs R buffer with 10 μM ionomycin (Calbiochem, San Diego, California, United States), 50 μM BAPTA-AM (Dojindo Laboratories, Kumamoto, Japan), and 10 mM EGTA (Dojindo Laboratories). Calcium saturation buffer was made of modified Krebs R buffer with 10 μM ionomycin and 10 mM $CaCl_2$. $[Ca^{2+}]$ measured by in situ calibration was calculated by the equation $[Ca^{2+}] = K'_d [(R - R_{min}) / (R_{max} - R)]^{(1/n)}$, where K'_d is the apparent dissociation constant corresponding to the calcium concentration and n is the Hill coefficient [55]. Because K'_d and n are constants but K'_d of RP in mitochondria is not known, we simply used the value of $(R - R_{min}) / (R_{max} - R)$ for the assessment of mitochondrial calcium level. The condition for imaging is basically similar to those described above.

Analysis of entire sequences of mtDNA. Total DNA was extracted from each cybrid using standard protocols. The entire mtDNA was sequenced as described [56]. A computer program, Sequencher version 4.1.1 (Gene Codes, Ann Arbor, Michigan, United States), was used to indicate possible SNP loci. For verification, visual inspection of each candidate SNP was carried out. At least two overlapping DNA templates amplified with different primer pairs were used for identification of each SNP. mtSNPs were identified by comparison with the revised Cambridge sequence (GI1944628) reported by Andrews et al. [57]. For all polymorphisms that resulted in changed amino acid sequence or those within rRNA or tRNA regions, averaged fluorescence ratios of mtRP were compared between genotypes by Mann-Whitney *U* test. This analysis was performed only when three or more cybrids had the same polymorphism. For statistical analysis, Mann-Whitney *U* tests were applied using SPSS software (SPSS, Tokyo, Japan).

Construction of pH indicator for measurements of mitochondrial matrix pH. *GFP* variants were prepared as described [57]. As a template, the original *GFP* mutation was employed. This template incorporates the mutation [38,58]. Mutations were verified by sequencing the entire gene. The *pH-GFP* [39] with polyhistidine tag at the N terminus was expressed in *Escherichia coli* JM109 (DE3) (Promega, Madison, Wisconsin, United States), purified, and spectroscopically characterized as described [55]. The gene for *mt pH-GFP* was amplified by PCR using the *GFP* variants as a template, with a forward primer containing *complex IV* mitochondrial target sequences and an MluI site, and a reverse primer containing an EcoRV site. The gene for *mt DsRed* was amplified by PCR using *pDsRed1-1 Mito* as a template with a forward primer containing a NotI site and a reverse primer containing a SalI site. The restricted *mt pH-GFP* product was subcloned in-frame into multiple cloning site I, and *mt DsRed* was subcloned into multiple cloning site II of the pBI bidirectional Tet vector (Clontech Laboratories, Mountain View, California, United States).

Transient expression of pH indicator in cybrid cell lines using the Tet system. To ensure the same expression levels of two genes, *mt pH-GFP* and *mt DsRed*, the bidirectional Tet expression vector was used in Tet-Off Gene expression systems [40,41]. The pBI bidirectional Tet expression vector contains a "bidirectional" promoter composed of a tetracycline-response element flanked by two minimal cytomegalovirus promoters in opposite orientations [42]. To induce these two genes, the other vector expressing the tetracycline-controlled transactivator under the cytomegalovirus promoter control was cotransfected.

Cybrids were grown in DMEM (Sigma-Aldrich) supplemented with 10% Tet system-approved FBS (Clontech), 100 U penicillin, and 100 μg/ml streptomycin. The cells were grown on dishes 35 mm in diameter to about 80% confluence. The cells were cotransfected with Tet-Off vector (Clontech) and pBI-*(mt pH-GFP)*-*(mt DsRed)* (total 1 μg DNA/dish) using Lipofect AMINE PLUS (Invitrogen). After 2 d, mitochondrial matrix pH was measured in these cells.

Mitochondrial matrix pH measurements and in vivo calibration. Cybrids in modified Krebs R buffer were imaged at room temperature. The imaging system is described above. Imaging with mt pH-GFP/DsRed used two excitation filters (480DF10 and S565/25), a dichroic mirror for GFP/DsRed, and emission filters (525AF45 and S620/60).

It was confirmed that the fluorescence ratio (525 nm/620 nm) decreased after the treatment with FCCP (Sigma-Aldrich), suggesting that this set of fluorescent indicators is sensitive to the mitochondrial matrix pH.

For in situ calibration, cybrids were perfused with the following pH titration buffer (125 mM KCl, 20 mM NaCl, 0.5mM $CaCl_2$, 0.5 mM $MgCl_2$, and 25 mM pH buffer [MOPS was used for pH 7.0, HEPES for pH 7.5 and 8.0, and glycylglycine for pH 8.5]) [59]. All calibration experiments were carried out in the presence of 10 μM nigericin and 10 μM monensin (Sigma-Aldrich). After baseline measurements were recorded for several minutes, calibration was performed in vivo. The fluorescence ratio of 525 nm emission at 480 nm excitation to 620 nm emission at 565 nm excitation reflected the dynamics of mitochondrial matrix pH. Mitochondrial matrix pH was calculated by plotting the calibration curve of each cell.

Supporting Information

Figure S1. Effects of *8701A/10398A* and *8701G/10398G* on Basal Mitochondrial Calcium Levels Measured by mtRP

The *y* axis shows the basal mitochondrial calcium levels indicated by the value of $(R - R_{min}) / (R_{max} - R)$ measured by mtRP. In situ calibration for $[Ca^{2+}]$ uses the equation $[Ca^{2+}] = K'_d [(R - R_{min}) / (R_{max} - R)]^{(1/n)}$. R is the basal ratio of the 525 nm fluorescence at 480 nm to that at 410 nm. R_{min} is the ratio at free calcium. R_{max} is the ratio at saturating calcium. K'_d is the apparent dissociation constant. n is the Hill coefficient. Bars indicate the standard error of mean for each cybrid cell line.

Found at DOI: 10.1371/journal.pgen.0020128.sg001 (120 KB PDF).

Table S1. mtDNA Polymorphisms in Eight Cybrids

Found at DOI: 10.1371/journal.pgen.0020128.st001 (97 KB XLS).

Acknowledgments

We sincerely thank the members of the Laboratory for Cell Function and Dynamics at the RIKEN Brain Science Institute. We thank the

members of the Research Resource Center at the RIKEN Brain Science Institute, especially Mr. Miyazaki, for technical assistance. We thank Ms. Bonnie Lee La Madeleine and Dr. S. Takeda, and Dr. T. Yoshida for valuable suggestions on the manuscript.

Author contributions. TK conceived and designed the experiments. AK and KM performed the experiments. AK and TK analyzed the data. AK, KM, TN, SS, MT, MY, NK, AM, and TK contributed reagents/materials/analysis tools. AK and TK wrote the paper.

Funding. This work was supported by an Independent Investigator Award from the National Alliance for Research on Schizophrenia and Depression (NARSAD) to T.K., a grant from the Japanese Ministry of Health, Labour and Welfare, and a grant from Japanese Ministry of Education, Culture, Sports, Science and Technology.

Competing interests. The authors have declared that no competing interests exist.

References

1. Hansford RG, Zorov D (1998) Role of mitochondrial calcium transport in the control of substrate oxidation. Mol Cell Biochem 184: 359–369.
2. Cortassa S, Aon MA, Marban E, Winslow RL, O'Rourke B (2003) An integrated model of cardiac mitochondrial energy metabolism and calcium dynamics. Biophys J 84: 2734–2755.
3. Demaurex N, Distelhorst C (2003) Cell biology. Apoptosis—The calcium connection. Science 300: 65–67.
4. Hajnoczky G, Davies E, Madesh M (2003) Calcium signaling and apoptosis. Biochem Biophys Res Commun 304: 445–454.
5. Rizzuto R, Pinton P, Ferrari D, Chami M, Szabadkai G, et al. (2003) Calcium and apoptosis: Facts and hypotheses. Oncogene 22: 8619–8627.
6. Kaftan EJ, Xu T, Abercrombie RF, Hille B (2000) Mitochondria shape hormonally induced cytoplasmic calcium oscillations and modulate exocytosis. J Biol Chem 275: 25465–25470.
7. Medler K, Gleason EL (2002) Mitochondrial Ca(2+) buffering regulates synaptic transmission between retinal amacrine cells. J Neurophysiol 87: 1426–1439.
8. Weeber EJ, Levy M, Sampson MJ, Anflous K, Armstrong DL, et al. (2002) The role of mitochondrial porins and the permeability transition pore in learning and synaptic plasticity. J Biol Chem 277: 18891–18897.
9. Li Z, Okamoto K, Hayashi Y, Sheng M (2004) The importance of dendritic mitochondria in the morphogenesis and plasticity of spines and synapses. Cell 119: 873–887.
10. Anderson S, Bankier AT, Barrell BG, de Bruijn MH, Coulson AR, et al. (1981) Sequence and organization of the human mitochondrial genome. Nature 290: 457–465.
11. Goto Y, Nonaka I, Horai S (1990) A mutation in the tRNA(Leu)(UUR) gene associated with the MELAS subgroup of mitochondrial encephalomyopathies. Nature 348: 651–653.
12. Kobayashi Y, Momoi MY, Tominaga K, Momoi T, Nihei K, et al. (1990) A point mutation in the mitochondrial tRNA(Leu)(UUR) gene in MELAS (mitochondrial myopathy, encephalopathy, lactic acidosis and stroke-like episodes). Biochem Biophys Res Commun 173: 816–822.
13. Hess JF, Parisi MA, Bennett JL, Clayton DA (1991) Impairment of mitochondrial transcription termination by a point mutation associated with the MELAS subgroup of mitochondrial encephalomyopathies. Nature 351: 236–239.
14. Smeitink J, van den Heuvel L, DiMauro S (2001) The genetics and pathology of oxidative phosphorylation. Nat Rev Genet 2: 342–352.
15. Poulton J, Luan J, Macaulay V, Hennings S, Mitchell J, et al. (2002) Type 2 diabetes is associated with a common mitochondrial variant: Evidence from a population-based case-control study. Hum Mol Genet 11: 1581–1583.
16. Hutchin T, Cortopassi G (1995) A mitochondrial DNA clone is associated with increased risk for Alzheimer disease. Proc Natl Acad Sci U S A 92: 6892–6895.
17. van der Walt JM, Dementieva YA, Martin ER, Scott WK, Nicodemus KK, et al. (2004) Analysis of European mitochondrial haplogroups with Alzheimer disease risk. Neurosci Lett 365: 28–32.
18. Shoffner JM, Brown MD, Torroni A, Lott MT, Cabell MF, et al. (1993) Mitochondrial DNA variants observed in Alzheimer disease and Parkinson disease patients. Genomics 17: 171–184.
19. van der Walt JM, Nicodemus KK, Martin ER, Scott WK, Nance MA, et al. (2003) Mitochondrial polymorphisms significantly reduce the risk of Parkinson disease. Am J Hum Genet 72: 804–811.
20. Hueria C, Castro MG, Coto E, Blazquez M, Ribacoba R, et al. (2005) Mitochondrial DNA polymorphisms and risk of Parkinson's disease in Spanish population. J Neurol Sci 236: 49–54.
21. Ghezzi D, Marelli C, Achilli A, Goldwurm S, Pezzoli G, et al. (2005) Mitochondrial DNA haplogroup K is associated with a lower risk of Parkinson's disease in Italians. Eur J Hum Genet 13: 748–752.
22. Kato T, Kunugi H, Nanko S, Kato N (2001) Mitochondrial DNA polymorphisms in bipolar disorder. J Affect Disord 62: 151–164.
23. McMahon FJ, Chen YS, Patel S, Kokoszka J, Brown MD, et al. (2000) Mitochondrial DNA sequence diversity in bipolar affective disorder. Am J Psychiatry 157: 1058–1064.
24. Canter JA, Kallianpur AR, Parl FF, Millikan RC (2005) Mitochondrial DNA G10398A polymorphism and invasive breast cancer in African-American women. Cancer Res 65: 8028–8033.
25. Mims MP, Hayes TG, Zheng S, Leal SM, Frolov A, et al. (2006) Mitochondrial DNA G10398A polymorphism and invasive breast cancer in African-American women. Cancer Res 66: 1880; author reply 1880–1881.
26. Skuder P, Plomin R, McClearn GE, Smith DL, Vignetti S, et al. (1995) A polymorphism in mitochondrial DNA associated with IQ? Intelligence 21: 1–11.
27. Kato C, Umekage T, Tochigi M, Otowa T, Hibino H, et al. (2004) Mitochondrial DNA polymorphisms and extraversion. Am J Med Genet 128B: 76–79.
28. Tanaka M, Takeyasu T, Fuku N, Li-Jun G, Kurata M (2004) Mitochondrial genome single nucleotide polymorphisms and their phenotypes in the Japanese. Ann N Y Acad Sci 1011: 7–20.
29. Tanaka M, Gong J, Zhang J, Yamada Y, Borgeld HJ, et al. (2000) Mitochondrial genotype associated with longevity and its inhibitory effect on mutagenesis. Mech Ageing Dev 116: 65–76.
30. King MP, Attardi G (1989) Human cells lacking mtDNA: Repopulation with exogenous mitochondria by complementation. Science 246: 500–503.
31. Nagai T, Sawano A, Park ES, Miyawaki A (2001) Circularly permuted green fluorescent proteins engineered to sense Ca^{2+}. Proc Natl Acad Sci U S A 98: 3197–3202.
32. Filippin L, Magalhaes PJ, Di Benedetto G, Colella M, Pozzan T (2003) Stable interactions between mitochondria and endoplasmic reticulum allow rapid accumulation of calcium in a subpopulation of mitochondria. J Biol Chem 278: 39224–39234.
33. Frieden M, James D, Castelbou C, Danckaert A, Martinou JC, et al. (2004) Ca(2+) homeostasis during mitochondrial fragmentation and perinuclear clustering induced by hFis1. J Biol Chem 279: 22704–22714.
34. Llopis J, McCaffery JM, Miyawaki A, Farquhar MG, Tsien RY (1998) Measurement of cytosolic, mitochondrial, and Golgi pH in single living cells with green fluorescent proteins. Proc Natl Acad Sci U S A 95: 6803–6808.
35. Porcelli AM, Ghelli A, Zanna C, Pinton P, Rizzuto R, et al. (2005) pH difference across the outer mitochondrial membrane measured with a green fluorescent protein mutant. Biochem Biophys Res Commun 326: 799–804.
36. Brini M, Pinton P, King MP, Davidson M, Schon EA, et al. (1999) A calcium signaling defect in the pathogenesis of a mitochondrial DNA inherited oxidative phosphorylation deficiency. Nat Med 5: 951–954.
37. Andrews RM, Kubacka I, Chinnery PF, Lightowlers RN, Turnbull DM, et al. (1999) Reanalysis and revision of the Cambridge reference sequence for human mitochondrial DNA. Nat Genet 23: 147.
38. Elsliger MA, Wachter RM, Hanson GT, Kallio K, Remington SJ (1999) Structural and spectral response of green fluorescent protein variants to changes in pH. Biochemistry 38: 5296–5301.
39. Matsuyama S, Llopis J, Deveraux QL, Tsien RY, Reed JC (2000) Changes in intramitochondrial and cytosolic pH: Early events that modulate caspase activation during apoptosis. Nat Cell Biol 2: 318–325.
40. Gossen M, Bujard H (1992) Tight control of gene expression in mammalian cells by tetracycline-responsive promoters. Proc Natl Acad Sci U S A 89: 5547–5551.
41. Gossen M, Freundlieb S, Bender G, Muller G, Hillen W, et al. (1995) Transcriptional activation by tetracyclines in mammalian cells. Science 268: 1766–1769.
42. Baron U, Freundlieb S, Gossen M, Bujard H (1995) Co-regulation of two gene activities by tetracycline via a bidirectional promoter. Nucleic Acids Res 23: 3605–3606.
43. Mizuno H, Sawano A, Eli P, Hama H, Miyawaki A (2001) Red fluorescent protein from *Discosoma* as a fusion tag and a partner for fluorescence resonance energy transfer. Biochemistry 40: 2502–2510.
44. Bernardi P (1992) Modulation of the mitochondrial cyclosporin A-sensitive permeability transition pore by the proton electrochemical gradient. Evidence that the pore can be opened by membrane depolarization. J Biol Chem 267: 8834–8839.
45. Trounce IA, Kim YL, Jun AS, Wallace DC (1996) Assessment of mitochondrial oxidative phosphorylation in patient muscle biopsies, lymphoblasts, and transmitochondrial cell lines. Methods Enzymol 264: 484–509.
46. Kato T (2001) DNA polymorphisms and bipolar disorder. Am J Psychiatry 158: 1169–1170.
47. Sudoyo H, Suryadi H, Lertrit P, Pramoonjago P, Lyrawati D, et al. (2002) Asian-specific mtDNA backgrounds associated with the primary G11778A mutation of Leber's hereditary optic neuropathy. J Hum Genet 47: 594–604.
48. Tanaka M, Gong JS, Zhang J, Yoneda M, Yagi K (1998) Mitochondrial genotype and longevity. Lancet 351: 185–186.
49. Matsunaga H, Tanaka Y, Tanaka M, Gong JS, Zhang J, et al. (2001) Antiatherogenic mitochondrial genotype in patients with type 2 diabetes. Diabetes Care 24: 500–503.

50. Takagi K, Yamada Y, Gong JS, Sone T, Yokota M, et al. (2004) Association of a 5178C→A (Leu237Met) polymorphism in the mitochondrial DNA with a low prevalence of myocardial infarction in Japanese individuals. Atherosclerosis 175: 281–286.
51. Dato S, Passarino G, Rose G, Altomare K, Bellizzi D, et al. (2004) Association of the mitochondrial DNA haplogroup J with longevity is population specific. Eur J Hum Genet 12: 1080–1082.
52. Niemi AK, Moilanen JS, Tanaka M, Hervonen A, Hurme M, et al. (2005) A combination of three common inherited mitochondrial DNA polymorphisms promotes longevity in Finnish and Japanese subjects. Eur J Hum Genet 13: 166–170.
53. Bentlage HA, Chomyn A (1996) Immunoprecipitation of human mitochondrial translation products with peptide-specific antibodies. Methods Enzymol 264: 218–228.
54. Nishino I, Kobayashi O, Goto Y, Kurihara M, Kumagai K, et al. (1998) A new congenital muscular dystrophy with mitochondrial structural abnormalities. Muscle Nerve 21: 40–47.
55. Miyawaki A, Llopis J, Heim R, McCaffery JM, Adams JA, et al. (1997) Fluorescent indicators for Ca^{2+} based on green fluorescent proteins and calmodulin. Nature 388: 882–887.
56. Tanaka M, Hayakawa M, Ozawa T (1996) Automated sequencing of mitochondrial DNA. Methods Enzymol 264: 407–421.
57. Sawano A, Miyawaki A (2000) Directed evolution of green fluorescent protein by a new versatile PCR strategy for site-directed and semi-random mutagenesis. Nucleic Acids Res 28: E78.
58. Wachter RM, Elsliger MA, Kallio K, Hanson GT, Remington SJ (1998) Structural basis of spectral shifts in the yellow-emission variants of green fluorescent protein. Structure 6: 1267–1277.
59. Ormo M, Cubitt AB, Kallio K, Gross LA, Tsien RY, et al. (1996) Crystal structure of the *Aequorea victoria* green fluorescent protein. Science 273: 1392–1395.

害による不妊の一部にセプチン系の異常が潜んでいる可能性を探索している．セプチンをマーカーとした蛍光抗体法により，精子無力症のうち25%もの症例で輪状小体形成不全を認めたが，正常対照群では皆無であった（15および未発表）．精子の形態には著しい種差のあることが知られているが，マウスだけでなくヒトでもセプチンリングは正常な鞭毛運動の必要条件のようである．セプチンリングの有無は，ヒト精子無力症の診断・分類基準として特異性が高いだけでなく，死滅あるいは凍結保存した検体でも明確に判定できることから，治療法選択や臨床研究に有用と考えられる．輪状小体形成不全を伴う精子無力症の原因がセプチン遺伝子の変異によるものかどうかは，臨床家グループが中心となって検討を進めている．

おわりに

セプチンの生物学は酵母の遺伝学に端を発する生命科学の一分野に過ぎないが，冒頭に挙げた先人たちの洞察に違わず，がん研究との接点は増え続けている．そればかりでなく，神経系や生殖系の疾患に密接に関与することも明らかになった．セプチンの医学・生物学的重要性を示す事例は今後ますます増えると予想されるが，現時点での生化学的知見はアクチンやチューブリンとは比較にならないほど少ない．これは研究の歴史が浅いことに加えて，研究の進展を妨げるいくつかの要因によるところが大きい．例えば，均質な複合体の精製が困難なこと，脱重合条件が不明なこと，特異的阻害剤がないこと，不規則な重合性によって構造解析が困難なことなどである．謎に包まれたこのGTP結合タンパク質の重合・脱重合サイクルの詳細と，その制御機構の解明につながるブレイクスルーが待ち望まれている．

1) Hartwell, L.H. (1967) *J. Bacteriol.* 93, 1662-1670
2) Byers, B. & Goetsch, L. (1976) *J. Cell Biol.* 69, 717-721
3) Kim, H.B., Haarer, B.K., & Pringle, J.R. (1991) *J. Cell Biol.* 112, 535-544
4) Neufeld, T.P. & Rubin, G.M. (1994) *Cell* 77, 371-379
5) Field, C.M., al-Awar, O., Rosenblatt, J., Wong, M.L., Alberts, B., & Mitchison, T.J. (1996) *J. Cell Biol.* 133, 605-616
6) Frazier, J.A., Wong, M.L., Longtine, M.S., Pringle, J.R., Mann, M., Mitchison, T.J., & Field, C. (1998) *J. Cell Biol.* 143, 737-749
7) Kinoshita, M. (2006) *Curr. Opin. Cell Biol.* 18, 54-60
8) Kinoshita, M., Kumar, S., Mizoguchi, A., Ide, C., Kinoshita, A., Haraguchi, T., Hiraoka, Y., & Noda, M. (1997) *Genes Dev.* 11, 1535-1547
9) Kinoshita, M. (2003) *J. Biochem.* 134, 491-496
10) Joberty, G., Perlungher, R.R., Sheffield, P.J., Kinoshita, M., Noda, M., Haystead, T., & Macara, I.G. (2001) *Nat. Cell Biol.* 3, 861-866
11) Kinoshita, M., Field, C.M., Coughlin, M.L., Straight, A.F., & Mitchison, T.J. (2002) *Dev. Cell* 3, 791-802
12) Spiliotis, E.T., Kinoshita, M., & Nelson, W.J. (2005) *Science* 307, 1781-1785
13) Hall, P.A. & Russell, S.E. (2004) *J. Pathol.* 204, 489-505
14) Kinoshita, A., Noda, M., & Kinoshita, M. (2000) *J. Comp. Neurol.* 428, 223-239
15) Ihara, M., Kinoshita, A., Yamada, S., Tanaka, H., Tanigaki, A., Kitano, A., Goto, M., Okubo, K., Nishiyama, H., Ogawa, O., Takahashi, C., Itohara, S., Nishimune, Y., Noda, M., & Kinoshita, M. (2005) *Dev. Cell* 8, 343-352

木下 專
（京都大学大学院医学研究科 先端領域融合医学研究機構 生化学・細胞生物学グループ，
科学技術振興機構 戦略的創造研究推進事業 さきがけ）

Emerging roles for the septin family of GTP-binding proteins in mitosis and cellular morphogenesis

Makoto Kinoshita (Biochemistry and Cell Biology Unit, HMRO, Kyoto University Graduate School of Medicine, Yoshida Konoe, Sakyo, Kyoto 606-8501, Japan; PRESTO, Japan Science & Technology Agency)

今，蛍光タンパク質で何ができるか？

はじめに

GFP（緑色蛍光タンパク質，以下そのファミリー全体を総称する場合は，単に「蛍光タンパク質」と呼ぶ）がなんら補因子を必要とせず，遺伝子導入するだけで生細胞内に蛍光を造り出せることが証明され，Scienceの表紙に華々しくデビューしたのが1994年．その後10年以上の歳月が流れた．その間GFPへの変異導入や様々な動物種からの類似遺伝子のクローニングにより，可視光域をほとんど網羅する波長変異体が開発されてきた．さらに，GFPの発色団の物理化学的特性やGFPが蛍光物質であるという特性を生かした様々な技術が開発されてきた．今や，興味あるタンパク質や細胞を蛍光標識したり，調べたい遺伝子プロモーターの下流に蛍光タンパク質遺伝子をつなげて細胞

に導入し，生きた状態で遺伝子の活性化を蛍光でモニターする等々のオーソドックスな利用に留まらず，タンパク質間相互作用やタンパク質機能の発現を時間的・空間的に可視化したり，光照射によりタンパク質の機能を破壊して，その生理機能を解析することも可能になってきた．これらの多くの技術を自分の研究に生かさない手はない．そこで，本稿では蛍光タンパク質を用いて今何ができるのかを，代表的な手法を幾つか挙げて解説したい．

1. GFP発色団の電荷状態を利用したバイオセンサー

GFPの発色団（*p*-hydroxybenzyliden imidazolinone）はフェノール環を持ち，その水酸基の電荷状態に応じて異なる波長の光を吸収する．つまり，非イオン化状態では395 nmに，イオン化状態では470 nmに吸収ピークが現れ，両状態間の平衡がどちらにずれるかによって，吸収スペクトルが変化する．この電荷状態は発色団とそれを取り巻く様々なアミノ酸の間の複雑な電荷相互作用によって調節されており，例えば，203番目のスレオニンをイソロイシンに置換すると非イオン化状態へ平衡がシフトするため，395 nmの吸収が優位になり（Sapphire），65番目のセリンをスレオニンに置換するとイオン化状態へ平衡がシフトし，470 nmの吸収が優位になる（EGFP）．

タンパク質の構造変化やタンパク質間相互作用を発色団の電荷状態の変化に結びつけることができるならば，GFPの吸収スペクトルの変化を観察することによって，タンパク質の構造変化やタンパク質間相互作用を測定できるかもしれない．この発想に基づき，BairdらはCa^{2+}指示薬camgarooを開発した[1]．camgarooはGFPの黄色変異体（YFP）の144番目と145番目のアミノ酸の間にCa^{2+}結合タンパク質であるcalmodulin（CaM）を挿入したキメラタンパク質で，CaMのCa^{2+}結合に伴う立体構造変化により発色団近傍の電荷相互作用が変化し，その結果Ca^{2+}有無での蛍光強度が7倍変化する．

一方，筆者らはYFPの円順列変異体（cpYFP）を用いることにより，Ca^{2+}指示薬pericamを開発した[2]．円順列変異とはおおもとのタンパク質の内部に新たなN末端とC末端を設定し，もとのC末端とN末端を適当なアミノ酸配列で連結する変異である．pericamは145番目のアミノ酸を新たなN末端とするcp145YFPのN末端とC末端に，M13ペプチドとCaMを連結している．M13とCaMのCa^{2+}依存的な相互作用に伴う立体構造変化を利用して，発色団の電荷状態を変化させることを原理とする．蛍光強度がCa^{2+}の結合により8倍増加するflash-pericam，逆に7倍減少するinverse-pericam，励起スペクトルが変化するratiometric-pericamの3種類が開発されている．最近では，円順列変異蛍光タンパク質を用いたタンパク質リン酸化のバイオセンサーも作成されており[3]，本手法による様々なバイオセンサーの登場を期待したい．

GFP発色団の周辺環境はGFP自身の二量体化によっても影響を受けるらしい．De AngelisらはGFP発色団の電荷状態がGFP同士の二量体化によって影響を受ける結果，395 nmと475 nmの吸収強度比が変化することを発見し，この性質を利用してタンパク質間相互作用を可視化するPRIM（proximity imaging）法を開発した[4]．この方法を用いて，免疫抑制剤であるFK506に依存したFKBPのホモダイマー化が生きた細胞内で観察されているが，応用例が乏しい．

2. 分割GFPによるタンパク質間相互作用の可視化

HuらはGFPをN末端側とC末端側の二つの断片に分けて発現させると，何れの断片も蛍光性を持たないが，それぞれの断片に相互作用するタンパク質を繋げると，タンパク質間相互作用を介してGFPが再構成され，蛍光発光することを見出した[5]．BiFC（bimolecular fluorescence complementation）と呼ばれる本方法により，bZIPタンパク質ファミリーとRelタンパク質ファミリー間の相互作用が培養細胞を用いて観察されている．さらに彼らはGFP波長変異体（青，シアン，緑，黄）のN末端側，C末端側断片を様々に組み合わせることによって，スペクトルが異なる7種類の蛍光タンパク質ができることを突き止め，多種類のタンパク質間相互作用を一つの細胞内で観察する方法も開発している[6]．

BiFC法はタンパク質間相互作用を可視化する方法だけでなく，特異的な組織を標識する方法としても注目されている．通常，ある組織を蛍光タンパク質で標識する場合，その組織に特異的な遺伝子プロモーターの制御下で蛍光タンパク質を発現させる．しかしながら，全ての組織に特異的な遺伝子プロモーターが見出されているわけではない．そこでZhangらは組織特異性が異なる二つの遺伝子プロモーターを利用し，それぞれの活性がオーバーラップする領域に蛍光タンパク質を発現させることができないかと考え，BiFC法を応用した．mec-3プロモーターにN末端側GFPを，egl-44プロモーターにC末端側GFPを連結して線虫に遺伝子導入することで，たった二つのFLP神経だけを蛍光標識することに成功している[7]．